universität wien

DIPLOMARBEIT

Titel der Diplomarbeit

Genetic Analysis of Rap1 GTPase Function in Vertebrate Axis Extension and Somitogenesis

angestrebter akademischer Grad

Magistra der Naturwissenschaften (Mag. rer.nat.)

Verfasserin:	Simone Lackner
Matrikel-Nummer:	0205274
Studienrichtung (lt. Studienblatt):	Molekulare Biologie A 490
Betreuer:	Dr. Scott A. Holley

Wien, am 11.September 2009

für meinen Bruder Michael Lackner

„ Jeder Mensch mit einer neuen Idee ist ein Spinner,
bis die Idee Erfolg hat “

Mark Twain

Acknowledgement

I am very grateful to Dr. Scott A. Holley for giving me the opportunity to come to Yale, to work in his lab, for his great support and the 'endless' monday-meetings with his enormous scientific knowledge input.
I would like to thank Dörthe Jülich for her generous patience while teaching me the methods I needed, for numerous interesting discussions and helpful critics on my manuscript.
Thank you, to Timothy Brand for trying to answer all this never-ending continuous questions, for informative discussions and useful critics on my manuscript.
I also would like to thank Nicolas Dray, who took my fear of the confocal-microscope and taught me with endless patience how to use it.
Thanks to all the members of the Holley lab for the warm welcome to the lab, to Yale and the United States of America and for the great scientific as well as cultural exchange.

My gratitude to 'the lunch group' - my friends at Yale, who where there for me in good and the best times as well as in bad and the *wors(es)t* times.

Special thanks to my friends back home for their across-the-sea lasting friendship and support.

Most importantly, I deeply want to thank my parents Monika and Ernst Lackner:
Danke, dass ihr mich nie eingeschränkt habt und ich immer den Dingen ‚nachforschen' durfte, die mich interessiert haben!

Summary

Somitogenesis is the process in which the segmental precursors of the skeletal muscle and vertebral column are generated during vertebrate embryogenesis. Somites form in an anterior to posterior sequence along both sides of the notochord concomitant with the posterior elongation of the embryo. Continuous migration of mesodermal progenitor cells in the tail bud drives axial growth. A patterning mechanism called the somite clock creates oscillating gene expression in the presomitic mesoderm. These oscillations create a segmental pattern that governs somitogenesis. Stabilisation of the oscillations in the anterior PSM establishes segment polarity, leading to morphological segmentation. Somites form as somite border cells undergo mesenchymal-to-epithelial transition. Simultaneously, the boundary cells assemble an extracellular matrix composed of Fibronectin, which stabilizes the border and is necessary for the completion of somite morphogenesis. Fibronectin is the ligand of the transmembrane protein Integrinα5. During somitogenesis, Integrinα5 appears to be activated via 'inside-out' signalling to ensure segmental Fibronectin matrix assembly. Studies indicate that Eph/Ephrin signalling has an impact on somite border formation and furthermore suggest a correlation to Integrinα5. Literature suggests that Eph/Ephrin signalling may regulate the small GTPase Rap1, which was shown to be involved in Integrin-mediated cell-adhesion via 'inside-out' signalling during T-cell activation. Here, the starting hypothesis was that Eph/Ephrin signalling activates the small GTPase Rap1, which leads to Integrinα5 activation and clustering. In turn, Integrin assembles ubiquitously secreted Fibronectin dimers into an insoluble extracellular matrix, which stabilizes the somite border.

To investigate the hypothesis, morpholino mediated knockdown experiments, *in situ* hybridisation and immunochemistry to characterize the function of the two isoforms *rap1a* and *rap1b* and of one *rapGEF* were performed. Consistent with the hypothesis that Rap1 regulates Integrinα5 during somitogenesis, a genetic interaction between Rap1 signalling and Integrinα5 was found, whereas the link between Eph/Ephrin signalling, Rap1 signalling and Integrinα5 activation still has to be established.

Zusammenfassung

Die Bildung von Somiten, den segmentären Vorläufern der Skelettmuskulatur und der Wirbelsäule, ist ein Prozess während der Embryogenese in der Gruppe der Wirbeltiere. Somiten bilden sich der Reihe nach von anterior zu posterior an beiden Seiten der Chorda dorsalis, wobei der Embryo gleichzeitig nach posterior wächst. Mesodermale Zellen wandern dabei kontinuierlich in die Schwanzknospe und führen dadurch zum Längenwachstum des Embryos. Ein Strukturierungsmechanismus, die so genannte ‚somite clock' erzeugt oszillierende Genexpression im pre-somitischen Mesoderm. Diese Oszillationen erzeugen ein Segmentmuster, wodurch die Somitogenese reguliert wird. Stabilisierung der Oszillationen im anterioren PSM führt zur Segmentpolarität und folglich zur morphologischen Segmentierung. Somiten bilden sich, wenn die äußersten Zellen einer zukünftigen Somite eine mesenchymal-to-epithelial transition (MET) durchlaufen, während die angrenzenden Zellen eine extrazelluläre Matrix aus Fibronektin assemblieren. Die Fibronektin Matrix ist wichtig zur Stabilisierung der Somitenabgrenzung und für die Vervollständigung der Somitenmorphogenese. Fibronektin ist der Ligand des Transmembranproteins Integrinα5. Während der Somitogenese scheint Integrinα5 durch ‚inside-out' Signalisierung segmentäre Fibronektin Matrix Assemblierung sicherzustellen. Studien deuten darauf hin, dass Eph/Ephrin Signalisierung einen Einfluss auf die Entstehung von Somitenabgrenzung hat, und weisen weiters auf einen Zusammenhang mit Integrinα5 hin. Die Fachliteratur schlägt vor, dass Eph/Ephrin Signalisierung vielleicht die kleine GTPase Rap1 reguliert. Es wurde gezeigt, dass Rap1 an der Integrin-vermittelten Zelladhäsion durch ‚inside-out' Signalisierung während der T-Zellen Aktivierung beteiligt ist. Die Anfangshypothese war daher, dass Eph/Ephrin Signalisierung die kleine GTPase Rap1 aktiviert, was zur Integrinα5 Aktivierung und Clusterbildung führt. Integrinα5 wiederum assembliert allgegenwärtige sekretierte Fibronektin Dimere in eine unlösbare extrazelluläre Matrix, wodurch die Somitenabgrenzung stabilisiert wird.

Um diese Hypothese zu untersuchen und die Funktion der zwei Isoformen *rap1a*, *rap1b* und eines *rapGEF*s zu charakterisieren, wurden Morpholino vermittelter Knockdown, *in situ* Hybridisierung und Immunohistochemie durchgeführt. Übereinstimmend mit der Hypothese, dass Rap1 Integrinα5 während der Somitogenese reguliert, wurde ein genetisches Zusammenspiel zwischen Rap1 Signalisierung und Integrinα5 aufgewiesen, wobei aber die

Verknüpfung des Eph/Ephrin Signalisierung, des Rap1 Signalisierung und der Integrinα5 Aktivierung noch zu klären bleibt.

Table of Contents

1. Introduction

Somitogenesis is the process by which the developing trunk and tail of the vertebrate embryo gets divided into a series of metameric segments called somites. These mesodermal segments form sequentially in bilateral pairs flanking the notochord in an anterior to posterior manner concomitant with the posterior elongation of the embryo (Figure 1). This segmentation process provides the basic pattern to guide further development of the embryonic body. Somites give rise to the bone and cartilage of the adult trunk, the skeletal muscles and the dermis on the dorsal side of the body. Moreover, an anterior-posterior organisation of the embryo's body is generated, within somite cells are able to contribute to the development of the nervous system and the vasculature. The total number of somites, or the resultant number of vertebrae is species-specific, but varies widely from one species to another (Richardson et al. 1998). For instance, snakes can have more than 300 of vertebrae (Gomez et al. 2008), whereas the zebrafish, *Danio rerio* completes somitogenesis with around 30 somite pairs by 24 hours post fertilisation (hpf) (Kimmel et al. 1995).

1.1. Somitogenesis in Zebrafish, *Danio rerio*

Fate mapping of the zebrafish blastula shows that the axial mesoderm, including the notochord develops from the embryonic shield, the dorsal margin of the blastula (Figure 2.A), whereas somites develop from the paraxial mesoderm, the ventral-lateral mesoderm. During gastrulation mesodermal cells ingress along the blastoderm margin (Figure 2.A) in response to Nodal and BMP (bone morphogenetic protein) signalling (Schier 2003, Pourquié 2001), whereas Nodal specifies the cell fate of the dorsal-lateral margin and BMP of the ventral margin (Szeto and Kimelman 2006). The mesoderm, which gives rise to the anterior somites of the trunk is generated via convergence and extension movements of cells derived from the dorsal-lateral blastoderm margin (Figure 2.B). Cells from the ventral margin fail to undergo convergence extension and ventrally contribute to the developing tail bud (Figure 2.B), giving rise to the most posterior somites and providing the cells necessary for tail elongation (Myers et al. 2002). Additionally, some cells form a dorsal-medial domain above the notochord,

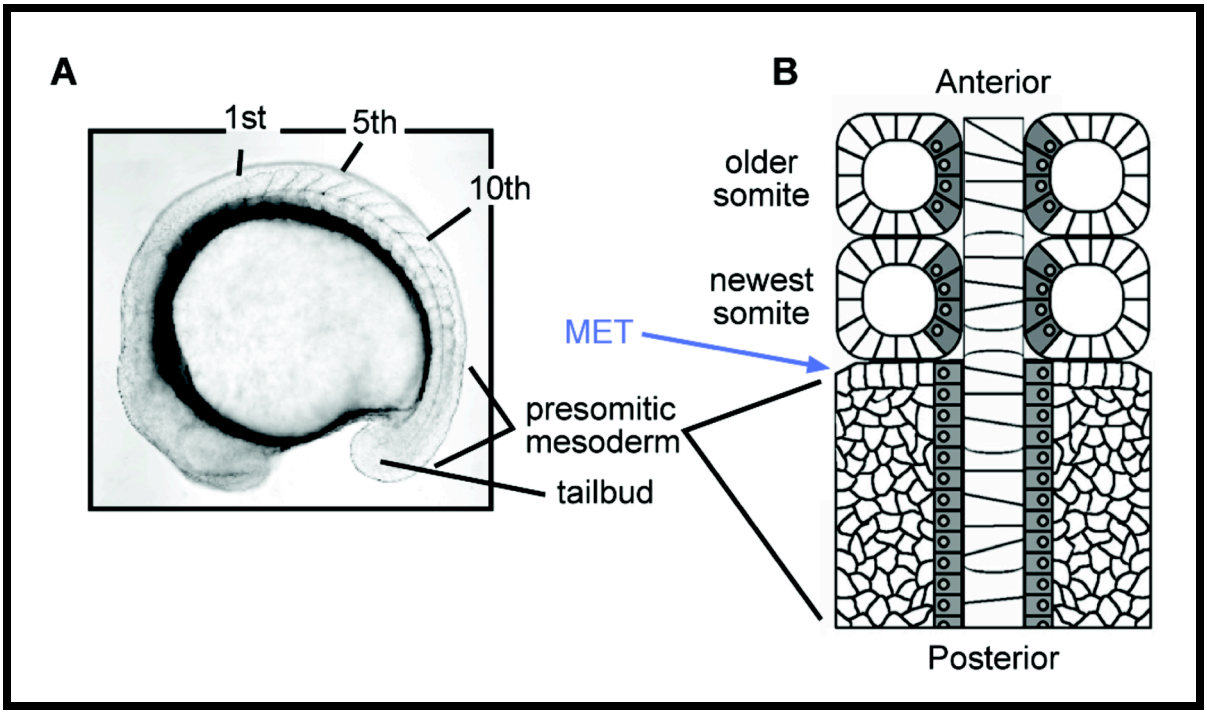

Figure 1. Somite morphogenesis in zebrafish

(A) Live zebrafish embryo at 15-somite stage. 1st, 5th and 10th somites are labelled. **(B)** Schematic longitutudinal section of the anterior presomitic mesoderm, the notochord and the recently formed somites. A mesenchymal-to-epithelial transition (MET) occurs along the nascent somite borders. The adaxial cells are shadowed.
Figure **(A)** and **(B)** were provided with permission by Scott Holley.

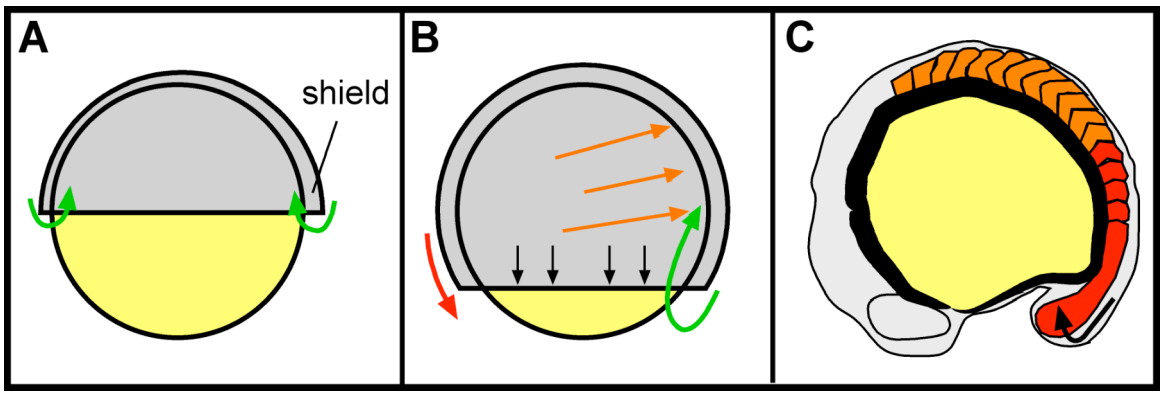

Figure 2. Gastrulation movements in zebrafish

(A) The shield stage characterizes the onset of gastrulation and marks the future dorsal side of the embryo. Cells ingress at the blastoderm margin (green arrows), which causes a local thickening at the dorsal blastoderm margin forming the shield. **(B)** Epiboly stage: Convergence-extension movements (orange arrows) lead to further thickening of the dorsal side concomitant with epiboly toward the vegetal pole (black arrows). Involution at the dorsal margin continues (green arrow) while cells at the ventral margin (red arrow) move toward the ventral pole forming the future tail bud. **(C)** Anterior somites (orange) form from cells migrated via convergence-extension, whereas posterior somites (red) form from a combination of ventral derived cells and cells from the dorsal medial domain (black arrow) that migrates into the tail bud as the embryo extends.
Figure **(A)**, **(B)** and **(C)** were provided with permission by Andrew Mara (Mara 2008).

which migrates ventrally into the tail bud as the embryo extends posteriorly (Figure 2.C) (Kanki and Ho 1997).

Morphological segmentation of the paraxial mesoderm starts 10.5hpf. New somite pairs are created at a constant rate, approximately every 30 minutes (at 28°C) beginning at the end of gastrulation until around 30 somite pairs in similar size and shape have been formed. Approximately, every five to six cells an intersomitic furrow is generated (Holley et al. 2000) as mesodermal cells in the most anterior presomitic mesoderm (PSM) undergo mesenchymal-to-epithelial transition (MET) (Figure 1).

1.2. The 'Clock and Wavefront' model

Given the resolution in somite number and size, somitogenesis seems to be subjected to a precise control mechanism. In 1976, Cook and Zeeman proposed that somites form in a process illustrated as the clock and wavefront model, which was given a molecular identity in the last few years (Cook and Zeeman 1976). The molecular existence of such an oscillator was first shown with the discovery of the oscillating expression of the chick gene *c-hairy1* (Palmeirim et al. 1997), subsequently the *hairy* homologue *her-1* was shown to oscillate in the zebrafish PSM (Holley et al. 2000). Additionally, studies indicate that the clock is regulated via the Notch signalling pathway, but it is still unclear if Notch is the core component of the oscillator or just simply necessary to produce the oscillating gene expression (Holley at el. 2002). The clock causes cells of the morphological un-segmented PSM to undergo repeated cycles of transcriptional activation and repression of several Notch pathway genes for instance *her-1*. Furthermore, Notch signalling synchronises oscillations of these genes, thereby creating a striped expression pattern that moves like a wave from the posterior to the anterior through the cells of the PMS (Figure 3). Simultaneously, the so-called wavefront governs maturation of the PSM cells in an anterior to posterior manner and determines the transition from the cell's immature to the mature state. Molecular studies suggest that the expression level of *fgf8*, a member of the *fibroblast growth factor* (*fgf*) family regulates the wavefront (Dubrulle et al. 2001, Sawada et al. 2001). *fgf8* is expressed in a gradient throughout the PSM, with the highest expression level at the most posterior and the lowest level at the most anterior (Figure 4). PSM cells exposed to high levels of *fgf8* are kept in an immature state such that they can respond to signals provided by the clock. Once cells

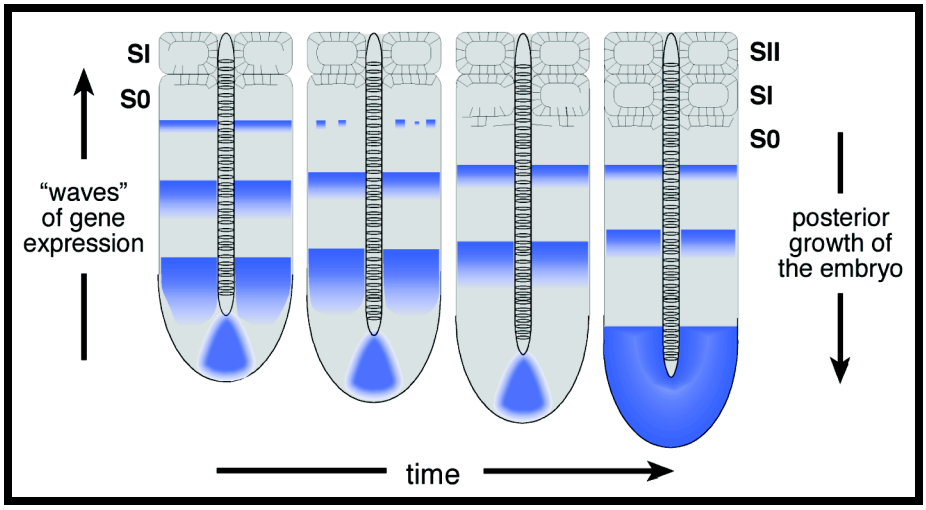

Figure 3. The clock mediated oscillating gene expression

One embryo at four different time points is shown. SI labels the most recently formed somite and S0 labels the region comprising the next somite. The segmentation clock causes genes in the morphological un-segmented PSM to undergo oscillating gene expression in an anterior to posterior manner (blue) while the tail extends posteriorly. Upon stabilisation of the oscillations in the anterior PSM, cells undergo MET and form a new somite.
Figure 3 was provided with permission by Scott Holley.

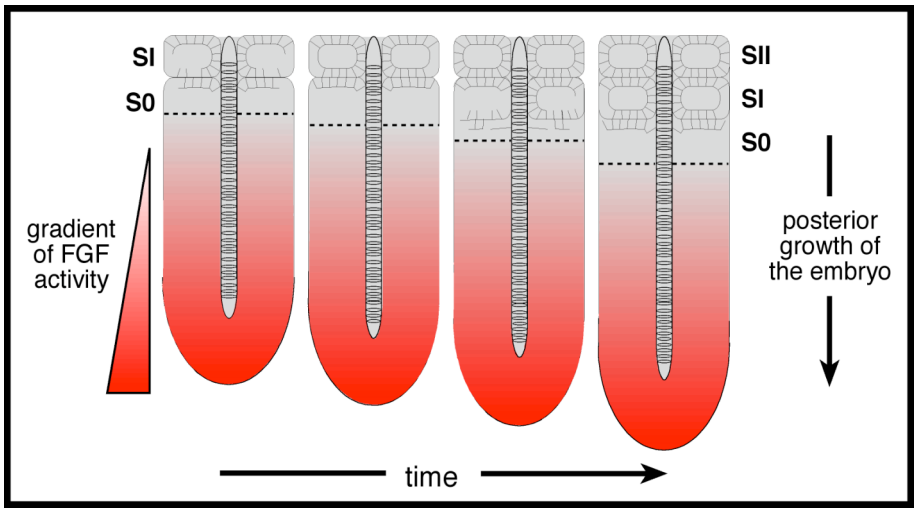

Figure 4. FGF gradient, the wavefront interacts with the clock

One embryo at four different time points is shown. SI labels the most recently formed somite and S0 labels the region comprising the next somite. The wavefront is controlled via the FGF gradient (red). As the tail bud extends, the gradient moves posteriorly, allowing cells in the most anterior PSM (dashed line) to fix their segmental position. Oscillation of gene expression is stabilized and cells are induced to undergo MET to form a new somite.
Figure 4 was provided with permission by Andrew Mara (Mara 2008).

escape the *fgf8* gradient to enter a more mature state in the anterior PSM, they become competent to fix their segmental identity. Thus, the clock interacts with the wavefront and the oscillation of gene expression gets stabilized, providing the spatiotemporal information required for somite border formation.

1.3. Somite polarity

The spatiotemporal information generated by the clock and wavefront determines the position of a presumptive somite boundary. Notch signalling induces the expression of segment polarity genes like *mesp-b* (Sawada et al. 2000), *ripply-1* (Kawamura et al. 2005), *ephrinB2a* and *ephA4* (Barrios et al. 2003), which leads to a segmental pattern resulting in the establishment of segment polarity within the PSM and presumptive somites. Furthermore, the establishment of segment polarity leads to the onset of morphological segmentation (Saga and Takeda 2001).

Presumptive somites can be subdivided into an anterior and posterior half implicated through differential expression of the segment polarity genes. A presumptive intersomitic furrow is formed every five to six cells posterior to an already existing somite border via juxtaposed cell-cell communication and changes of cell adhesion. The receptor EphA4, a member of the Eph family of transmembrane receptor tyrosine kinases and its ligand EphriB2a were shown to have a role as intercellular signalling molecules within this process (Durbin et al. 1998, Durbin et al. 2000). Furthermore, EphA4 and EphrinB2a were shown to be involved in various other developmental processes for instance in the repulsion and attraction process during axon guidance (Mellitzer et al. 1999) or in cell sorting and boundary formation during hindbrain segmentation (Xu et al. 1995, Cooke et al. 2001). A characteristic feature of the Eph/Ephrin complex is their ability to generate bidirectional signals that affect both the receptor-expressing cell and the ligand-expressing one (Pasquale 2005). Accordingly, signalling downstream of Eph receptors is called forward signalling, whereas signalling downstream of the ligand EphrinB2a is called reverse signalling (Pasquale 2008). During zebrafish somite furrow formation, the juxtaposed expression pattern of *ephA4* in the anterior half of the somite and *ephrinB2a* in the posterior half, generates repulsion of anterior and posterior cell populations, followed by cell de-adhesion creating a boundary between the

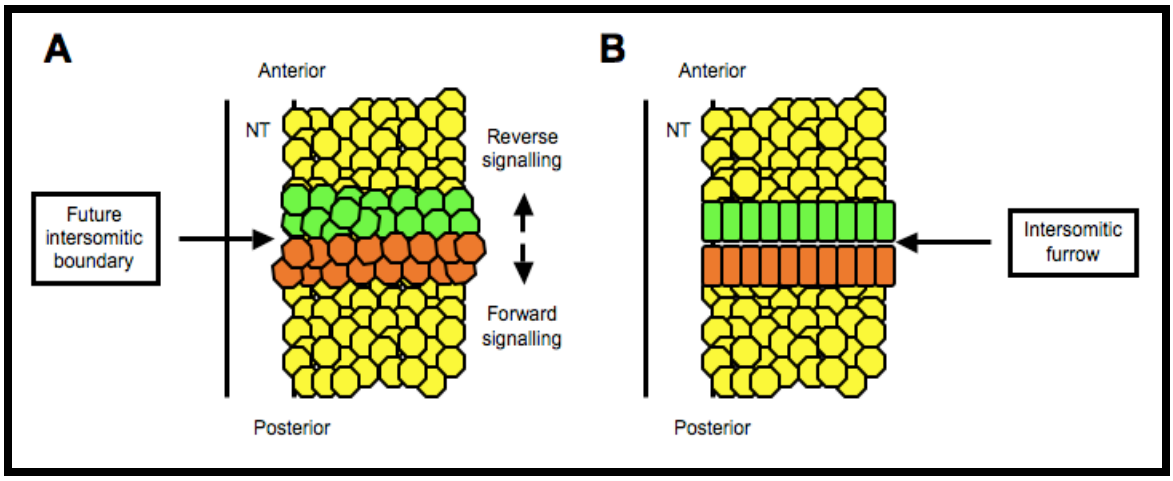

Figure 5. Eph/Ephrin signalling mediates mesenchymal-to-epithelial transition leading to intersomitic furrow formation

(A) Mesenchymal cells in green express EphrinB2a, whereas cells in orange express EphA4. Signalling downstream of EphA4 expressing cells is called Forward signalling, whereas signalling downstream of EphrinB2a expressing cells is called Reverse signalling. **(B)** The juxtaposed expression pattern of EphA4 and EphrinB2a generates repulsion of the anterior and the posterior cell population, followed by cell de-adhesion creating an intersomitic furrow as cells undergo MET. Boundary cells undergo changes associated with a mesenchymal-to-epithelial transformation from a polygonal to a columnar cell shape.
Figure **(A)** and **(B)** were adapted from Pasquale 2005.

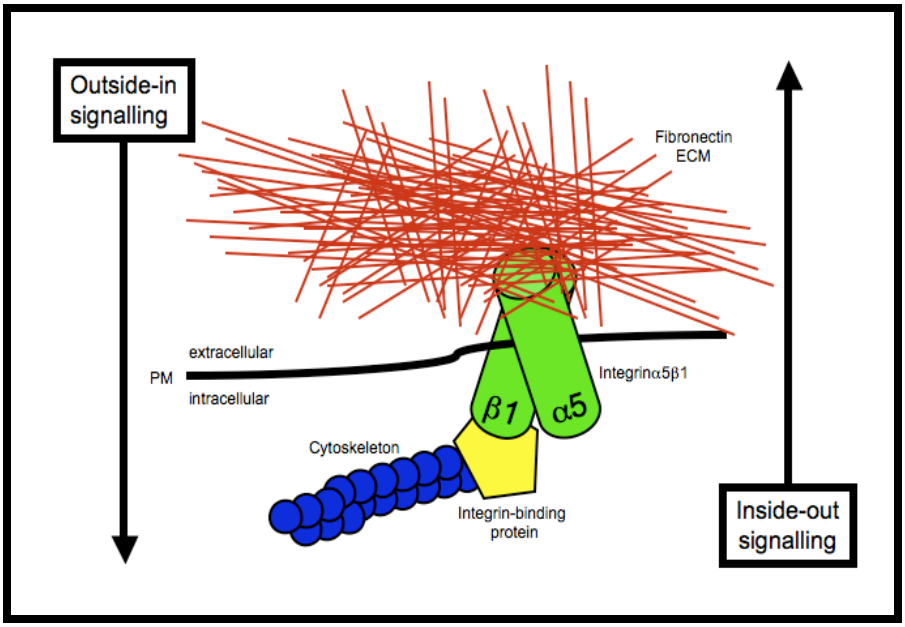

Figure 6. Integrin signalling

Integrinα5β1 links the ECM to the actin cytoskeleton and is able to relay bidirectional signals over the membrane. Via 'inside-out' signalling, Integrinα5β1 can activate the ECM and via 'outside-in' signalling it can affect changes of the cytoskeleton and of gene expression.

paraxial mesoderm cells (Barrios et al. 2003). Concomitantly, border cells undergo MET and mature somites form (Figure 5).
In summary, intersomitic furrow formation via MET is regulated by Eph/Ephrin signalling. Nevertheless, continuation of somite border morphogenesis requires additional signals.

1.4. Somite border morphogenesis

Epithelial morphology within a presumptive somite is generated via MET, whereas boundary cells undergo changes in shape associated with the transformation from a mesenchymal-polygonal to an epithelial-columnar shape (Figure 5). This process leads ultimately to an epithelial sphere with remaining mesenchymal cells at its inner core. Furthermore, changes in cell adhesive interactions and sub-cellular polarisation of organelles and proteins contribute to reveal a mature somite (Barrios et al. 2003). Simultaneously, the boundary cells assemble an extracellular matrix (ECM) composed of Fibronectin, which stabilizes the border and is necessary for the completion of somite border formation (George et al. 1993). Fibronectin dimers interact with receptors belonging to the Integrin superfamily of heterodimeric transmembrane proteins (Sonnenberg 1993). Integrins, composed of an α and a β subunit physically link the ECM to the actin cytoskeleton (Figure 6). Integrin-Fibronectin interaction promotes Fibronectin-Fibronectin association resulting in Fibronectin matrix accumulation in a process called fibrillogenesis (Schwarzbauer and Sechler 1999, Mao and Schwarzbauer 2005). Integrins can relay signals bidirectionally over the membrane via “inside-out” signalling to modify the ECM or via “outside-in” signalling to alter the structure of the cytoskeleton and affect gene expression (Figure 6). Integrinα5 was shown to be the primary receptor for Fibronectin matrix assembly (Hynes, 1994) and studies in cell culture suggest that its activation is necessary for Fibronectin matrix assembly (Mao and Schwarzbauer 2005). Recent studies suggest that Integrinα5 and the Notch signalling pathway act in concert to govern MET and Fibronectin matrix assembly during zebrafish somite formation (Jülich et al. 2005a). Nevertheless, the link between Integrinα5 and Eph/Ephrin signalling during somite border formation is still not clearly understood.

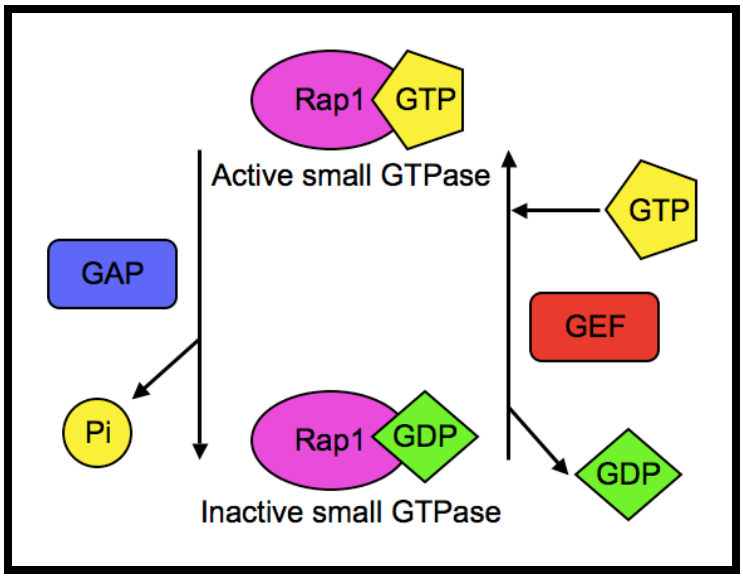

Figure 7. The small GTPase Rap1

The small GTPase Rap1 cycles between an active GTP-bound form and an inactive GDP-bound form. GAP (GTPase activating Protein) regulates GTP-hydrolysis and GEF (Guanine-nucleotide Exchange Factor) regulates GDP dissociation.

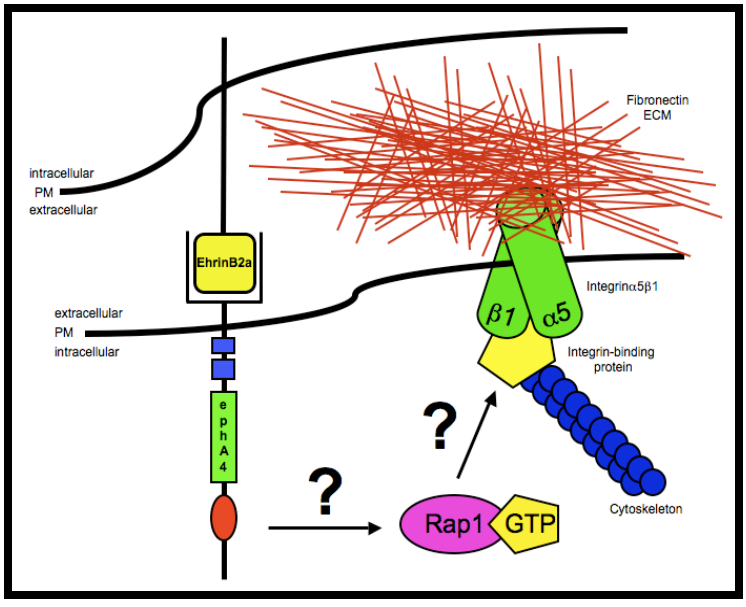

Figure 8. Model of 'inside-out' Integrin activation during zebrafish somite morphogenesis

In this model, Eph/Ephrin signalling could regulate via 'forward' signalling Rap1 GTPase function, which in turn could mediate via 'inside-out' signalling Integrin clustering. Integrin binds Fibronectin and promotes Fibronectin matrix formation.

1.5. Rap1 signalling – filling the gap?

Integrinα5 has been shown to cluster on the surface of somite boundary cells concomitantly with the initiation of somite border formation, while Fibronectin matrix assembly is detected around five to ten minutes later (Jülich et al. 2005a). Consequently, these two observations suggest that the initial Integrinα5 clustering along the nascent somite boundaries is not due Fibronectin mediated 'outside-in' signalling, but due to cytoplasmic, cell autonomous 'inside-out' signalling. Immunological studies suggest that the small GTPase Rap1 is involved in Integrin-mediated cell-adhesion via 'inside-out' signalling during T-cell immune response (Katagiri et al. 2003, Sebzda et al. 2002). Furthermore, experiments in cell culture have shown that Eph proteins regulate Integrin-mediated cell-adhesion (Huynh-Do et al. 1999) and that EphA4 can activate the small GTPase Rap1 (Aoki et al. 2004). However, conflicting data on the relationship between these signalling pathways exists and the literature suggests that Rap1 signalling can be found context dependent either activated or inhibited (Pasquale 2008).
The small cytoplasmic GTPase Rap1 is a monomeric G-protein, which exists in two isoforms, Rap1a and Rap1b, differing only in a few amino acids (Bos et al. 2001). Rap1 belongs to the Ras superfamily and like Ras GTPases, Rap1 cycles between an inactive GDP-bound and an active GTP-bound conformation (Figure 7). The kinetics of GTP hydrolysis and GDP dissociation are regulated by two classes of auxiliary proteins, the GTPase-activating proteins (GAPs) and the Guanine-nucleotide exchange factor (GEF) (Kinbara et al. 2003). Respectively, GAPs induce the hydrolysis of the bound GTP, whereas GEF facilitate the release of the bound nucleotide and allow more abundant GTP to bind. Rap1 was shown to be involved in several aspects of cell adhesion, including Cadherin-mediated cell junction formation (Price et al. 2004) and Integrin-mediated cell adhesion (Katagiri et al. 2003, Sebzda et al. 2002). Studies suggest that Rap1 mediates cellular signals that regulate Integrins from the inside of the cell, thereby mediating binding of cells to other cells (Kinbara et al. 2003).
These observations lead to our starting hypothesis, that Integrinα5 clustering could be due to Rap-mediated via 'inside-out' signalling. More broadly, Notch signalling functions to set up distinct expression domains of Eph/Ephrin signalling, which then could activate Rap1. Rap1 would then cause Integrinα5 clustering and consequently induce Fibronectin matrix formation (Figure 8).

1.6. Aim of the project

A large-scale mutant screen for zebrafish mutant embryos with anterior or/and posterior somite border formation defects was performed (Jülich et al. 2005a). Two mutant alleles of a gene named *before eight* (*bfe*), which caused anterior somite border defects, were identified and positional cloning of the locus revealed that the gene encodes *integrinα5* (Jülich et al. 2005a). While positional cloning the *bfe* locus, a *rapGEF* was identified on the same chromosome upstream of *integrinα5* and subsequently genetic interaction studies suggested a potential regulator role of RapGEF for Integrin activity (Jülich 2005c). Furthermore, the small GTPase Rap1 was shown to be required for normal tissue morphogenesis during *Drosophila* embryogenesis, linking the cytoskeleton to adherence junctions and therefore regulating adhesion-dependent cell shape changes and maintenance (Asha et al. 1999, Knox and Brown 2002). Studies in *Xenopus* and zebrafish suggested that Raps are involved in convergent extension movements during gastrulation downstream of non-canonical Wnt signalling and that Rap1 function is required for proper zebrafish tail elongation (Tsai et al. 2007). Recent studies revealed that Rap1 is also required to stabilize the epithelial cell-cell junctions of the zebrafish vasculature downstream of cerebral cavernous malformation (CCM) pathway genes (Gore et al. 2008). Summing up, these results suggest a conserved role of the Rap1 GTPase in regulating cell-cell junction formation during invertebrate and vertebrate development. Nonetheless, Rap1 had only been shown to regulate Integrins during vertebrate immune response. Hence, it was in our main interest to characterize the genetic function of Raps during zebrafish somitogenesis and subsequently determining the link between Eph/Ephrin and Integrin signalling during somite morphogenesis.

2. Results

2.1. Examination of the role of Rap1a, Rap1b and RapGEF during somite border morphogenesis

The complete coding sequence of zebrafish *rap1a* (Tsai et al. 2007, Strausberger et al. 2002, Thisse et al. 2001) and *rap1b* (Tsai et al. 2007, Song et al. 2004, Thisse et al. 2001) was isolated and for both a full-length sequence clone was generated. *rap1a* is located on chromosome 8 with six exons and a coding sequence of 558bp. *rap1b* is located on chromosome 4, composed of six exons and comprises a coding sequence of 555bp. The coding sequence of zebrafish *rapGEF* was known only partially (Sanger zK27M20 BAC), whereas the start codon was not yet identified. Therefore, a 5'rapid amplification of cDNA ends (RACE) was performed using Clontech's SMART^{TM} RACE cDNA Amplification Kit to isolate the complete 5'sequence of the target transcript (described in Materials and Methods 4.3.). A full-length cDNA of *rapGEF* was generated and the complete coding sequence was cloned. *rapGEF* is located on chromosome 23 upstream of *integrinα5* and spans approximately 70kbp of genomic sequence in 27 exons to produce a coding sequence of 2.6kbp (Appendix 5.1-5.2).

To analyse the gene expression pattern of *rap1a*, *rap1b* and *rapGEF*, full-length riboprobes via *in vitro* transcription were generated. *in situ* hybridisation using embryos at several developmental stages before and after gastrulation revealed that all three genes seem to be ubiquitously expressed during early zebrafish development (Figure 1-3). Furthermore, to analyse Rap1b and RapGEF protein localisation, a cellular GFP fusion protein was cloned to the N-terminus of *rap1b* and *rapGEF*. A GFP tagged mRNA was generated via *in vitro* transcription and injected into wild-type embryos. Rap1b-GFP seemed to be ubiquitously expressed, whereas RapGEF-GFP localisation was not detectable at all, which might be due to miss-folding and subsequent degradation of the approximately 3.4kbp RapGEF-GFP fusion protein.

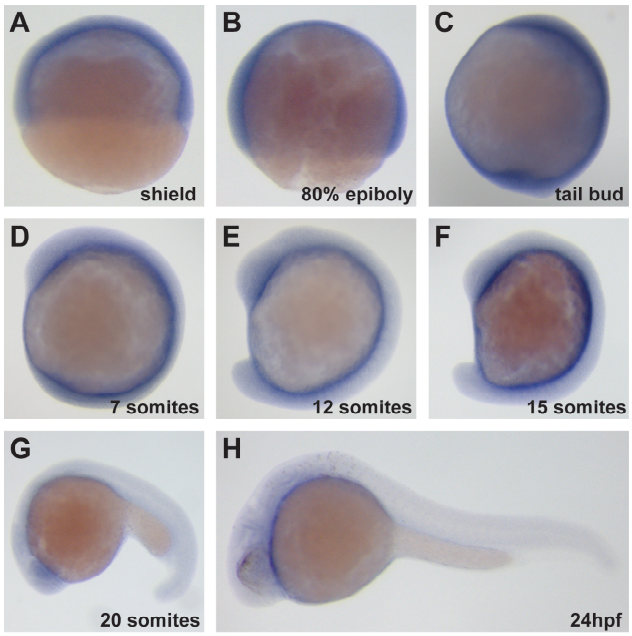

Figure 1. *rap1a* gene expression pattern

Zebrafish *rap1a* expression of various stages during early development. *rap1a* was ubiquitously expressed. (A) shield stage (B) 80% epiboly (C) tail bud stage (D) 7 somite stage (E) 12 somite stage (F) 15 somite stage (G) 20 somite stage (H) 24hpf

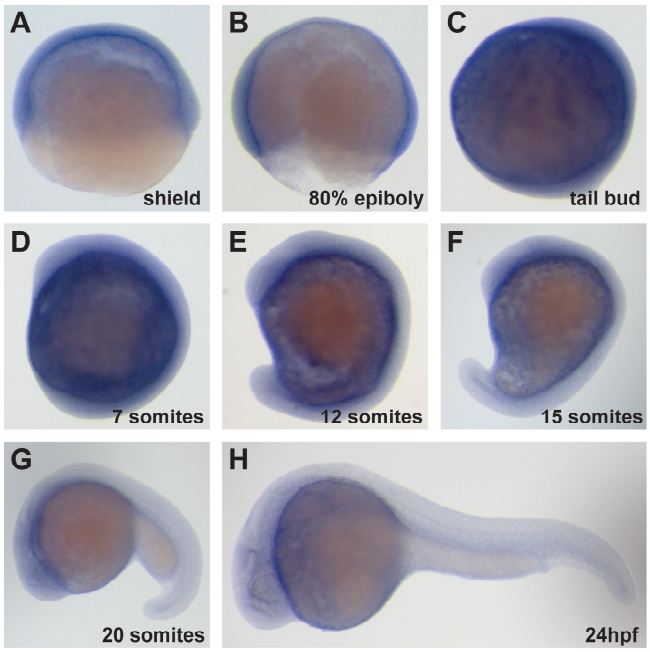

Figure 2. *rap1b* gene expression pattern

Zebrafish *rap1b* expression of various stages during early development. *rap1b* was ubiquitously expressed with increased expression in the tail bud tip and the adaxial cells during somitogenesis. (A) shield stage (B) 80% epiboly (C) tail bud stage (D) 7 somite stage (E) 12 somite stage (F) 15 somite stage (G) 20 somite stage (H) 24hpf

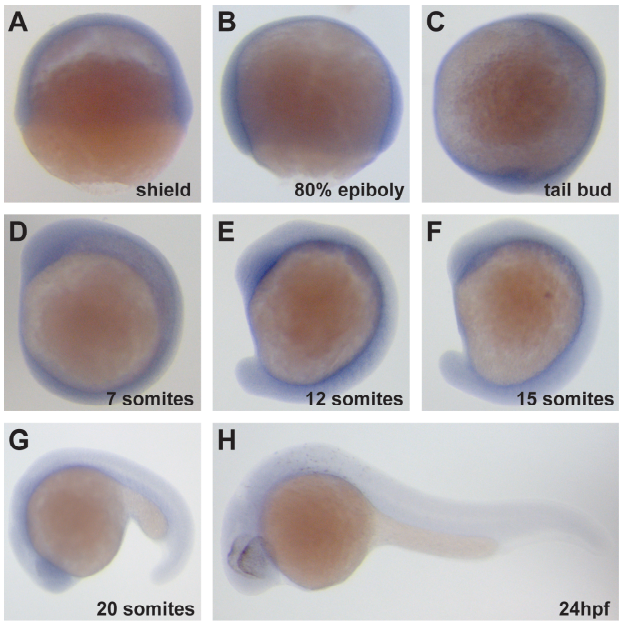

Figure 3. *rapGEF* gene expression pattern

Zebrafish *rapGEF* expression of various stages during early development. *rapGEF* was ubiquitously expressed with increased expression in the tail bud tip and the adaxial cells during somitogenesis. (A) shield stage (B) 80% epiboly (C) tail bud stage (D) 7 somite stage (E) 12 somite stage (F) 15 somite stage (G) 20 somite stage (H) 24hpf

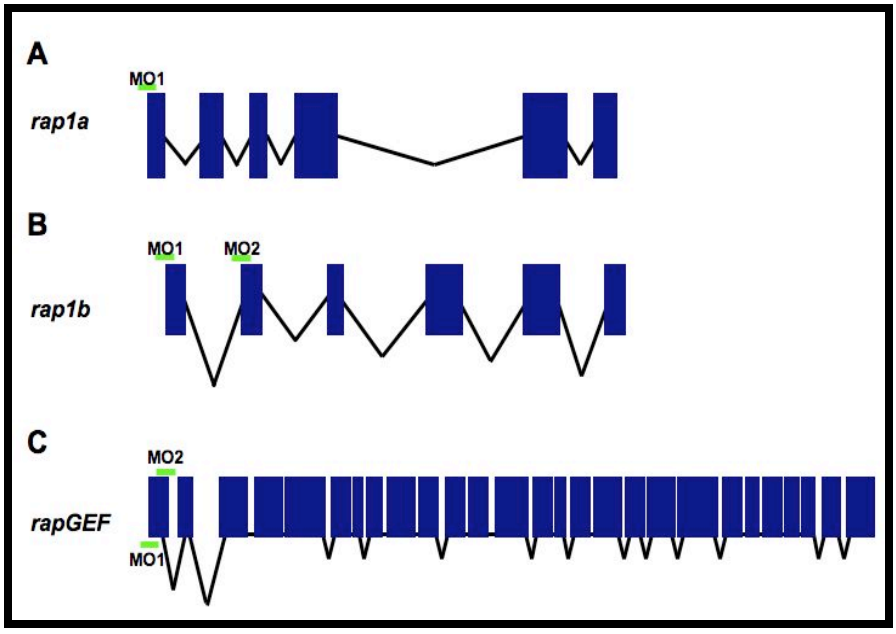

Figure 4. Gene map of *rap1a*, *rap1b* and *rapGEF*

Gene map of *rap1a* (A), *rap1b* (B) and *rapGEF* (C). *rap1a* (A) and *rap1b* (B) are encoded by six exons and *rapGEF* (C) by 27 exons. MO1 stands for translation-blocking morpholino. MO2 stands for splice-blocking morpholino.

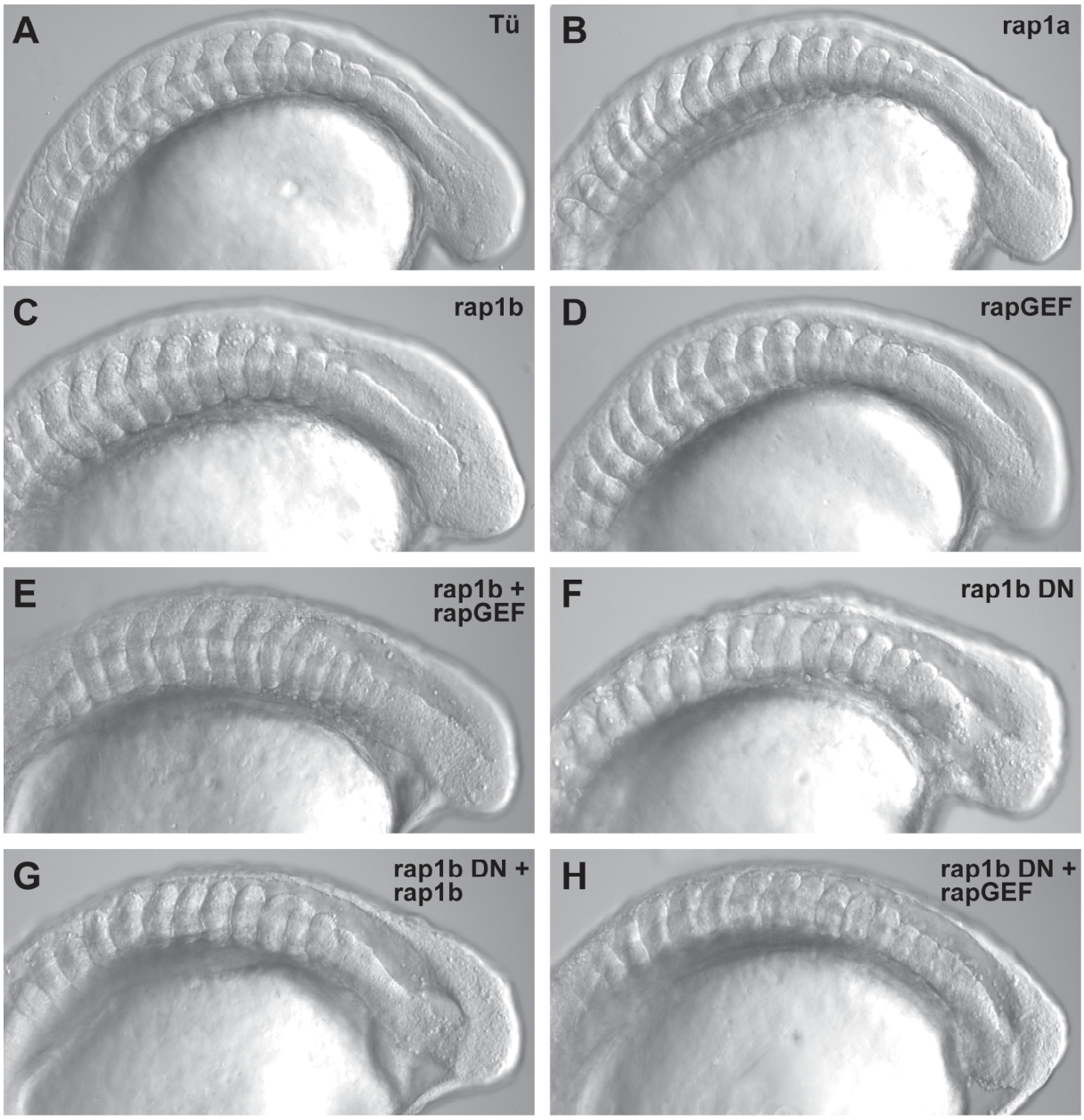

Figure 5. Inhibition of *rap1a*, *rap1b* and *rapGEF* function in wild-type embryos

Morpholino mediated knockdown of *rap1a* (B), *rap1b* (C) and *rapGEF* (D) in wild-type embryos (A) led to anterior-posterior axis elongation defects. The phenotype was enhanced via double knockdown of *rap1b* and *rapGEF* (E). Injection of rap1b DN mRNA led to similar defects (F). Co-injection of rap1b DN mRNA with *rap1b* (G) or *rapGEF* (H) morpholino led to synergetic effects.

To characterize *rap1a*, *rap1b* and *rapGEF* function during early zebrafish development, loss-of-function studies via morpholino mediated gene knockdown were performed. To knockdown the function of *rap1a* and *rap1b*, translation-blocking morpholinos (Tsai et al. 2007) were designed (Figure 4.A-B). In case of *rapGEF*, the start codon was not known at this point, thus a splice-blocking morpholino was designed (Figure 4.C), which should prevent splicing at a specific splice junction between the first exon and the first intron. Knockdown of *rap1b* and *rapGEF* in wild-type zebrafish embryos generated anterior-posterior axis extension defects and a minor effect on the somites, in shape and size. No obvious morphological effects on the somite border formation were observed (Figure 5.C-D). The tail elongation defect included a thickened layer of cells at the dorsal side of the tail bud, which was milder in *rapGEF* than in *rap1b* knockdowns (Figure 5.C-D). Knockdown of *rap1a* produced similar but weaker defects as *rap1b* and *rapGEF* knockdowns (Figure 5.B). Their phenotypes were consistent with the previous studies (Tsai et al. 2007). Double knockdown of both *rap1b* and *rapGEF* in wild-type embryos generated an enhanced axis extension and tail elongation defect (Figure 5.E). This synergy suggested that *rap1b* and *rapGEF* are both involved in the same process during zebrafish axis elongation. To examine the specificity of the morpholino-mediated knockdown phenotypes, a dominant-negative (dn) Rap1b (S17N) mRNA construct (rap1b DN) was generated via PCR mediated site-directed mutagenesis (Gabig et al. 1995). Injection of dn-Rap1b(S17N) mRNA into wild-type embryos mirrored the *rap1b* and *rapGEF* knockdown phenotypes, featuring the characteristic tail elongation defect and an anterior-posterior extension defect (Figure 5.F). Furthermore, a synergetic effect via co-injecting dnRap1b(S17N) mRNA with the *rap1b* translation-blocking morpholino and the *rapGEF* splice-blocking morpholino was generated. Embryos exhibited in both cases strong enhancement of anterior-posterior axis extension and the tail elongation defect similar to the double knockdown of *rap1b* and *rapGEF* (Figure 5.E,G-H), emphasizing the specificity of the morpholino-mediated knockdown phenotype.

To further assess whether the morpholino-mediated knockdown phenotypes of *rap1b* and *rapGEF* are gene-specific and are not off-target phenotypes, additional morpholinos for *rap1b* and *rapGEF* were designed. Since after the 5'RACE, the start codon of *rapGEF* was finally known, a translation-blocking morpholino (*rapGEF-2*) was designed (Figure 4.C). To knockdown *rap1b*, a splice-blocking morpholino (*rap1b-2*) that should prevent splicing at the splicing site of the second exon and intron (Tsai et al. 2007) was generated (Figure 4.B). For both *rap1b* and *rapGEF*, similar phenotypes were reproduced via injecting translation-

blocking and splice-blocking morpholino independently. Additionally, synergetic effects between the translation-blocking and splice-blocking morpholino specific for one gene were tested, but due to issues with difficulties in interpreting the thresholds of injection concentrations the experiment was unsuccessful. Nevertheless, the gene-specificity of the splice-blocking morpholino against *rap1b* was verified via PCR (Appendix 5.7) and sequencing of an altered splice product (Appendix 5.3-5.6). The sequence of the altered splice product was around 70bp smaller than the wild-type target, missing the second exon completely and therefore confirming the specificity of the morpholino. The specificity of the splice-blocking morpholino against *rapGEF* was until now not successfully demonstrated due to issues with genomic DNA contamination during RNA isolation. Another approach was to test whether gene specific mRNA could rescue the morpholino-mediated phenotype. mRNA *in vitro* transcription of the complete coding sequence of the cloned genes *rap1b* and *rapGEF* was performed and the mRNA was injected into wild-type embryos. However, a gain-of-function phenotype of Rap1b mRNA injected into wild-type embryos and the high toxicity of RapGEF mRNA precluded the rescue experiment.

2.2. Testing for genetic interaction between Rap1b, RapGEF and Integrinα5

To investigate the genetic relationship between Integrinα5 and Rap1 signalling, the consequence of eliminating *rap1b* or *rapGEF* in *bfe/integrinα5* mutant embryos was examined. Previous studies have shown that the *bfe/integrinα5* mutant has a defect in anterior somite border maintenance (Jülich et al. 2005). Anterior somite borders are initially formed but during proceeding somitogenesis, the first 3-8 somite borders start to disappear whereas the posterior somite borders persist (Figure 6.B). Although knockdown of *rap1b* and *rapGEF* gene function in wild-type embryos did not cause a segmentation defect (Figure 5.C-D), knockdown of, either *rap1b* or *rapGEF* in the *bfe*/*integrinα5* mutant lead to a strong enhancement of the somite border defect similar to knockdown of *fibronectin* function in the *bfe/integrinα5* mutant (Jülich et al. 2005a), which even affected the more posterior somites, so that only 2-4 posterior somite borders were still maintained (Figure 6.C-F). Additionally, the double knockdowns also revealed strong enhancement of the tail elongation and anterior-posterior extension defect (Figure 6.C-F). Injection of dnRap1b(S17N) mRNA into the *bfe/integrinα5* mutant mirrored the *rap1b* and *rapGEF* knockdown phenotype (Figure 6.G), supporting morpholino efficiency. In conclusion, the synergistic effect generated via double knockdown suggested a genetic relationship between Integrinα5, Rap1b and RapGEF, supporting the idea that the small GTPase Rap1 might function in Integrinα5 'inside-out' signalling.

Due to the morphological changes triggered by the perturbation of the Rap1 signalling, investigation whether Rap1 signalling alone or together with the Integrinα5 affect the somite clock, cell polarity establishment or segmental patterning during somitogenesis, was performed. Therefore, the effect of *rap1a*, *rap1b* and *rapGEF* perturbation on mRNA expression was analysed by the clock or the clock-induced segmental pattern during zebrafish somitogenesis. To perform *in situ* hybridisation, riboprobes to detect *her-1* and *myo-D* were generated. *her-1*, the oscillating gene is expressed in the PSM whereas *myo-D* is expressed in a segmental pattern in the posterior half of each somite (Figure 7.A). However, *rap1a*, *rap1b* and *rapGEF* knockdown mutant embryos appeared only to have minor defects in the

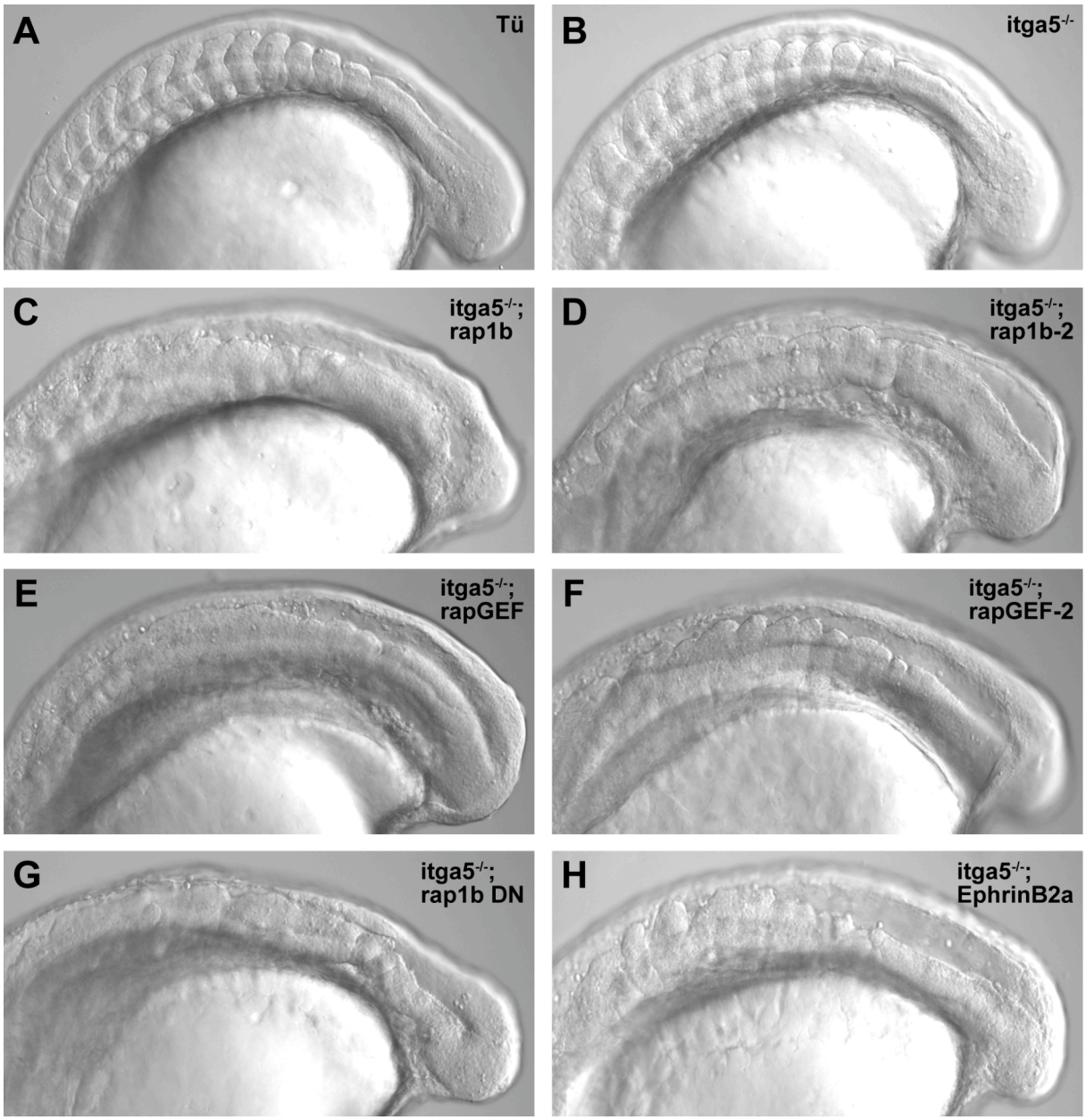

Figure 6. Inhibition of *rap1b*, *rapGEF* and *ephrinB2a* in *bfe/integrinα5* mutant embryos

Wild-type (A) zebrafish embryo at 12-15 somite stage. The *bfe/integrinα5* mutant (B) has defects in anterior somite border maintenance. Morpholino-mediated knockdown of *rap1b* (B-D) and *rapGEF* (E-F) in *bfe/integrinα5* mutant embryos enhanced somite border defect and anterior-posterior axis elongation defects. *rap1b* and *rapGEF-2* are translation-blocking morpholino, *rap1b-2* and *rapGEF* are splice-blocking morpholino. Injection of dnRap1b(S17N) into *bfe/integrinα5* mutant embryos (G) mirrored the phenotype of *rap1b* (C-D) and *rapGEF* (E-F) knockdown. Knockdown of *ephrinB2a* in *bfe/integrinα5* mutant embryos led to fused somite phenotype, where all somite borders are fused (H).

expression pattern of *her-1* and *myo-D*, as did wild-type embryos injected with the dnRap1b(S17N) mRNA (Figure 7.B-D,F). One exception was the double knockdown of *rap1b* and *rapGEF* in wild-type embryos, which showed spotty-ness in *her-1* expression, which might be due to aberrant cell movement associated with the strong tail elongation defect (Figure 5.E, 7.E). The *her-1* expression pattern was maybe slightly affected due to the morphological changes but the stripes could still be clearly seen, which suggested that the clock is functioning. The *myo-D* expression pattern, marking the segment border maintenance was comparable to the wild-type expression pattern and consistent with the morphological phenotype. Double knockdown of *rap1b* and *rapGEF* in wild-type embryos and knockdown of either *rap1b* or *rapGEF* in the *bfe/integrinα5* mutant, as well as *bfe/integrinα5* mutant embryo injected with dnRap1b(S17N) mRNA displayed a possible segment polarity defect, but did not show a big effect on the clock itself (Figure 7.E, G-K). The segmental expression pattern of *myoD* in the *bfe/integrinα5* mutant knockdowns appeared to be lost in the anterior somites, instead exhibiting an ambiguous expression consistent with the morphological phenotype of the anterior fused somites (Figure 6.C-G, 7.G-K).

rap1b and *rapGEF* effects on segment polarity establishment were examined using riboprobes for *mesp-b* and *ripply-1*. *mesp-b* is an early segment polarity marker expressed in the future anterior half of nascent somites (Figure 8.A) and *ripply-1* is another segment polarity marker, expressed in the anterior PSM and in the anterior half of the most recently formed somites (Figure 9.A). Knockdown of *rap1a*, *rap1b* and *rapGEF* in wild-type embryos did not show any distinguishable defects in *mesp-b* or *ripply-1* expression, compared to wild-type embryos (Figure 8.A-D, 9.A-D), except that the double knockdown of *rap1b* and *rapGEF* in wild-type embryos exhibited a sort of spotty-ness in *mesp-b* expression comparable to its *her-1* expression (Figure 7.E, 8.E). Knockdown of *rap1b* and *rapGEF* in *bfe/integrinα5* mutant embryo exhibited modest defects in the segmental expression pattern of both, *mesp-b* and *ripply-1* (Figure 8.F-G, 9.H-K).

ephA4 encodes a tyrosine kinase receptor expressed in the PSM and in the anterior half of each somite (Figure 10.A), shown to be involved in somite border formation. Single knockdown of *rap1a*, *rap1b* and *rapGEF* in wild-type embryos exhibited no significant defects in *ephA4* expression pattern (Figure 10.B-D), while double knockdown of *rap1b* and

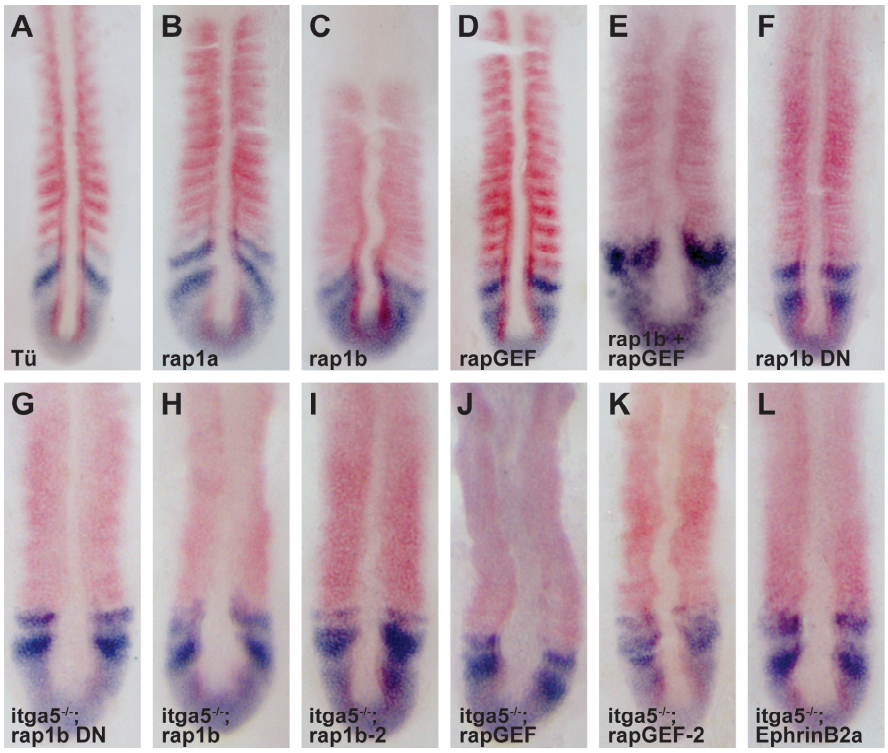

Figure 7. The segmentation clock and somite polarity

her-1 (blue) is an oscillating gene expressed in the PSM. *myo-D* (red) is expressed in a segmental pattern in the posterior half of each somite. Wild-type embryo (A). Knockdown of *rap1a* (B), *rap1b* (C), *rapGEF* (D) and *rap1b* together with *rapGEF* (E) in wild-type embryos appeared to cause only minor defects in the expression pattern of *her-1* and *myo-D*, so did wild-type embryos injected with dnRap1b(S17N) (F). Double.-knockdown of *rap1b* and *rapGEF* (E) in wild-type embryos showed a spotty-ness of *her-1* expression. Knockdown of *rap1b* (H-I), *rapGEF* (J-K), *ephrinB2a* (L) and injection of dnRap1(S17N) (G) in *bfe/integrinα5* mutant embryos showed only minor defects in *her-1* expression, whereas the segmental *myo-D* expression pattern was lost.

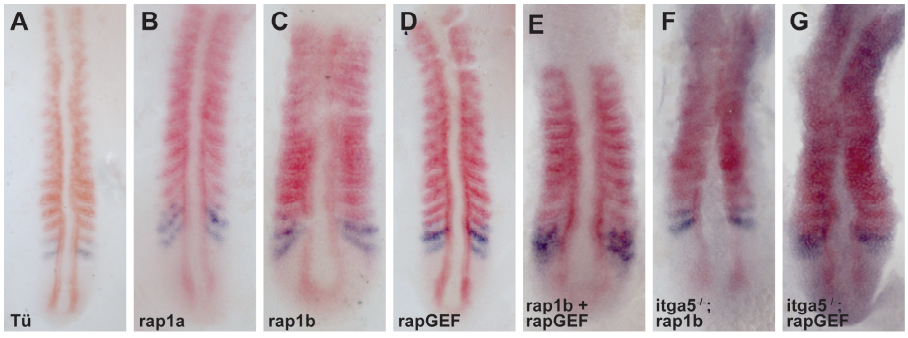

Figure 8. Segment polarity of nascent somites

mesp-b (blue) is a segment polarity marker expressed in the future anterior half of nascent somites. *myo-D* (red) is expressed in an segmental pattern in the posterior half of each somite. Wild-type embryo (A). Knockdown of *rap1a* (B), *rap1b* (C), *rapGEF* (D) in wild-type embryos and knockdown of *rap1b* (F) and *rapGEF* (G) in *bfe/integrinα5* mutant embryos caused no obvious defects in *mesp-b* expression pattern. Double-knockdown of *rap1b* and *rapGEF* (E) in wild-type embryos exhibited a spotty-ness of the *mesp-b* expression.

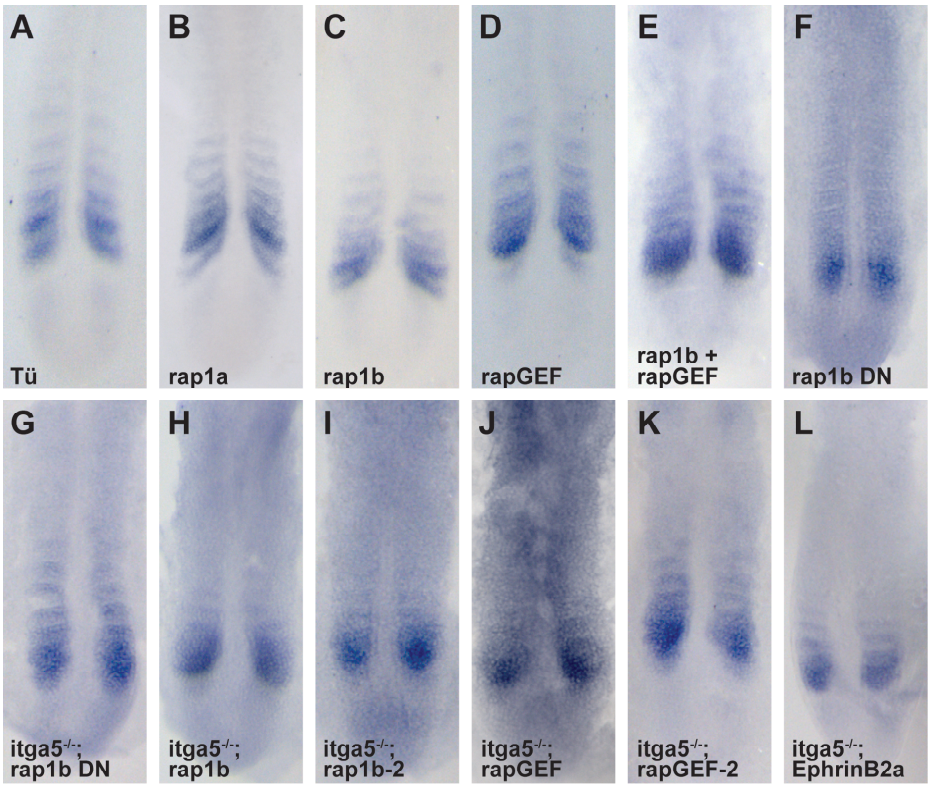

Figure 9. Segment polarity in recently formed somites

ripply-1 (blue) is expressed in a segmental pattern in the anterior PSM and in the anterior half of the most recently formed somite. Wild-type embryo (A). Knockdown of *rap1a* (B), *rap1b* (C), *rapGEF* (D) and *rap1b* together with *rapGEF* (E) in wild-type embryos appeared to cause only modest defects in the stripe expression pattern of *ripply-1*, as did wild-type embryos and *bfe/integrinα5* mutant embryos injected with dnRap1b(S17N) (F,G) and knockdown of *rap1b* (H-I), *rapGEF* (J-K) and *ephrinB2a* (L) in *bfe/integrinα5* mutant embryos.

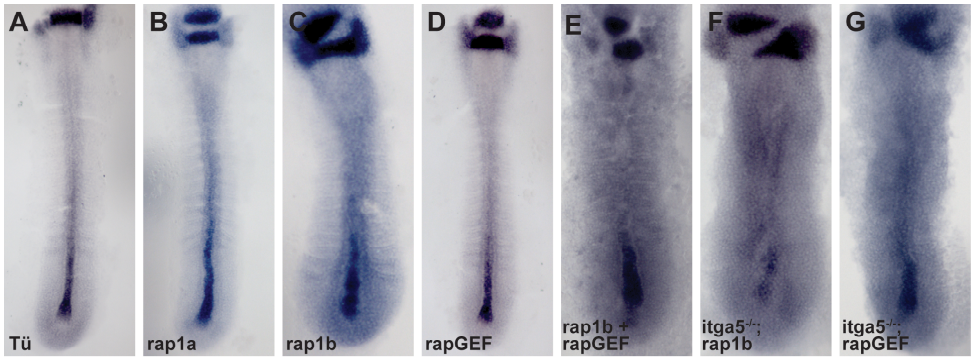

Figure 10. *ephA4* expression

epha4 (blue, purple) is a tyrosine kinase receptor expressed in the PSM and in the anterior half of each somite. Wild-type (A). Knockdown of *rap1a* (B), *rap1b* (C) and *rapGEF* (D) in wild-type embryos showed no significant defects in *ephA4* expression. Double-knockdown of *rap1b* and *rapGEF* (E) in wild-type embryos showed partial loss of the *ephA* expression pattern. Knockdown of *rap1b* (F) and *rapGEF* (G) in *bfe/integrinα5* mutant embryos showed complete loss of the ephA4 expression pattern.

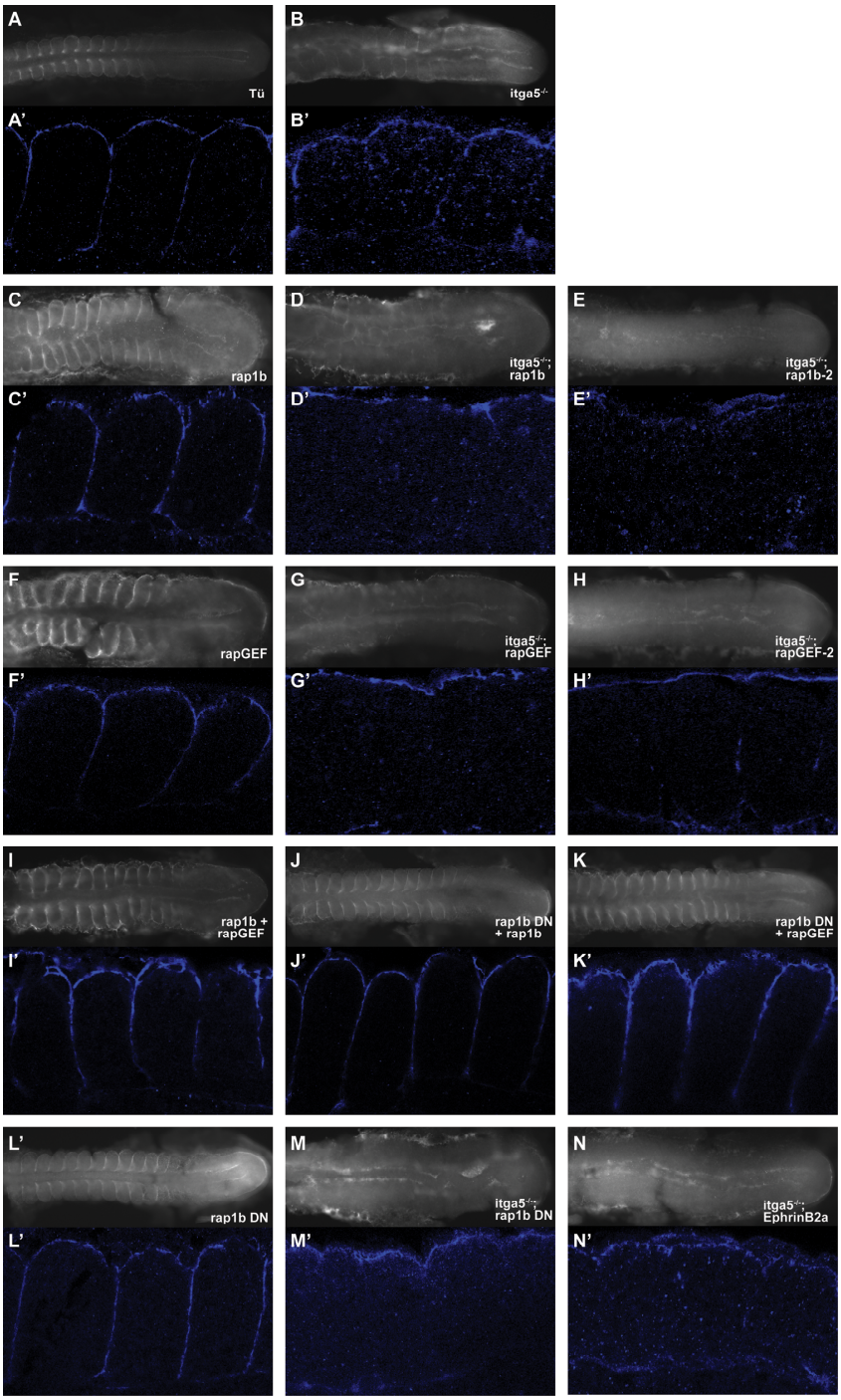

Figure 11. Fibronectin matrix assembly

Fibronectin (white, blue) immunostaining of embryos at 12-15 somite stage (A-N). Confocal images of the most posterior somites (A'-N'). Wild-type embryo (A, A'). Fibronectin matrix formation is affected in the posterior somites of a *bfe/integrinα5* mutant embryo (B, B'). Knockdown of *rap1b* (C, C') and *rapGEF* (F,F') and *rap1b* together with *rapGEF* (I,I') in wild-type embryos did not prevent segmental assembly of Fibronectin matrix, neither did single injection of dnRap1b(S17N) mRNA (L,L'), nor in combinations with *rap1b* (J,J') and *rapGEF* (K,K') morpholino. Knockdown of *rap1b* (D-E, D'-E') and *rapGEF* (G-H, G'-H') in *bfe/integrinα5* mutant embryos led to almost complete loss of Fibronectin matrix assembly, as did knockdown of *ephrinB2a* (N, N').

rapGEF in wild-type embryo showed partial loss of the *ephA4* expression pattern (Figure 10.E). However, knockdown of *rap1b* or *rapGEF* in the *bfe/integrinα5* mutant showed complete disruption of the *ephA4* expression pattern (Figure 10.F-G), which was consistent with their morphological phenotype (Figure 6.C-F).

To investigate the affects of the small GTPase Rap1b and RapGEF on Fibronectin matrix formation, which is induced around 5-10 minutes past Integrinα5 clustering (Jülich et al. 2005), embryos were immuno-stained using Fibronectin antiserum. Single and double knockdown of *rap1b* and *rapGEF* and injection of the dnRap1b(S17N) in wild-type embryo showed no effect on Fibronectin matrix formation (Figure 11.C, F, I-L), which was consistent with the morphological phenotype (Figure 5.C-F), in which somite borders were initially formed and maintained. In contrast, knockdown of *rap1b* and *rapGEF* in *bfe/integrinα5* mutant embryos resulted in almost a complete loss of Fibronectin accumulation (Figure 11.D-E, G-H, M), even at the 2-4 posterior established somite borders. Fibronectin could be detected at the lateral edge of the paraxial mesoderm and the notochord (Figure 11.D'-E', G'-H', M'), but not within the paraxial mesoderm, which was consistent with the morphological phenotype, where somite borders were initially formed but not maintained in the anterior somites (Figure 6.C-G). The results of the Fibronectin detection assay suggested that the small GTPase Rap1 promotes Fibronectin matrix formation, supporting the hypothesis that Rap signalling is involved in Integrinα5 'inside-out' signalling.

Studies have indicated that Eph/Ephrin signalling has an impact on somite border formation (Barrios et al. 2003) and furthermore suggest that it has a correlation to Integrinα5 (Koshida et al. 2005). Therefore, synergetic effects between Integrinα5 clustering and Eph/Ephrin signalling were investigated. Morpholino-mediated knockdown of *ephrinB2a* (Koshida et al. 2005), encoding a ligand of the receptor tyrosine kinase EphA4, in the *bfe/integrinα5* mutant, caused sever defects in somite boundary formation (Koshida et al. 2005), meaning a complete loss of somite boundaries (Figure 6.H). Somite borders were initially generated, but not maintained, neither anteriorly nor posteriorly, thereby enhancing the *bfe/integrinα5* mutant phenotype (Figure 6.B). Interestingly, knockdown of *ephrinB2a* also caused an anterior-posterior extension defect similar to the *rap1b* and *rapGEF* knockdowns (Figure 6.C-F, H).

Examination of the *her-1* expression pattern via *in situ* hybridisation did not show a big effect on the clock itself, as the expression stripes were still clearly visible (Figure 7.L). The *myo-D* expression pattern appeared to be lost in the anterior and posterior somites, exhibiting ambiguous expression consistent with the morphological phenotype of the fused somites.
However, knockdown of *ephrinB2a* did not show any great defect in the expression pattern of the segment polarity marker *ripply-1* (Figure 9.L).

Investigating Fibronectin matrix assembly, the embryos exhibited the same defect as other *bfe/integrinα5* double morphants, almost complete loss of Fibronectin in the paraxial mesoderm, with residual matrix at the lateral edge and in the notochord (Figure 11.N,N').

These results, suggested that there might be a genetic interaction between EphrinB2a and Integrinα5. Knockdown of *rap1b*, *rapGEF* and *ephrinB2a* in *bfe/integrinα5* mutant embryos, showed similar phenotypes in terms of defects in somite border maintenance, tail elongation, axis extension and loss of Fibronectin matrix assembly, which suggest that they all might be involved in the same signalling pathway during somite border morphogenesis. These observations support the hypothesis that Eph/Ephrin signalling functions upstream of Integrinα5 clustering and Fibronectin matrix formation via the small GTPase Rap1b and RapGEF during somite border formation and maintenance.

2.3. Determining the functional relationship between EphrinB2a, Rap1b, RapGEF and Integrinα5 signalling during somite border morphogenesis

Studies have indicated that Eph/Ephrin signalling is involved in somite border formation (Barrios et al. 2003), and furthermore suggest a correlation to Integrinα5 activation (Koshida et al. 2005). Additionally, literature suggests that Eph/Ephrin signalling may regulate the small GTPase Rap1 (Pasquale 2008) and Rap1 in turn has been implicated in the regulation of Integrin activity in the immune system (Abraham et al. 2003). Therefore, the direct or indirect genetic interaction between EphrinB2a and the Rap GTPase was investigated.

First, the expression pattern of EphrinB2a, the ligand of the receptor tyrosine kinase EphA4 was investigated via immunohistochemistry. EphrinB2a is expressed in the posterior half of each somite (Figure 12.A). Single and double knockdown of *rap1b* and *rapGEF* in wild-type embryos showed only minor defects on the expression pattern (Figure 12.B-C, E), whereas knockdown in the *bfe/integrinα5* mutant exhibited defects in the anterior expression pattern (Figure 12.D,F), exhibiting ambiguous expression correlated with the morphological phenotype (Figure 6.C-F).

Double knockdowns of *ephrinB2a* in combination with either the *rap1b* or *rapGEF* morpholino or the dnRap1b(S17N) mRNA were generated. All three combinations exhibited a similar phenotype characterized by an extremely short embryo body axis and strong necrosis in the head extending to the tail bud (Figure 13.D-F). The embryos showed no obvious somite border defect, though the most posterior somite borders are not easily to detect from the side view, whereas from the dorsal side weak somite borders are visible, which might be due to the extremely strong extension defect.

Fibronectin matrix formation of the EphrinB2a double morphants seemed to be weaker than in wild-type embryos (Figure 14.D-F), which could be due to the shortening body of the embryos. The Fibronectin matrix assembly along the somite borders (Figure 14.D'-F') showed no defect and was consistent with the morphological phenotype (Figure 13.D-F).

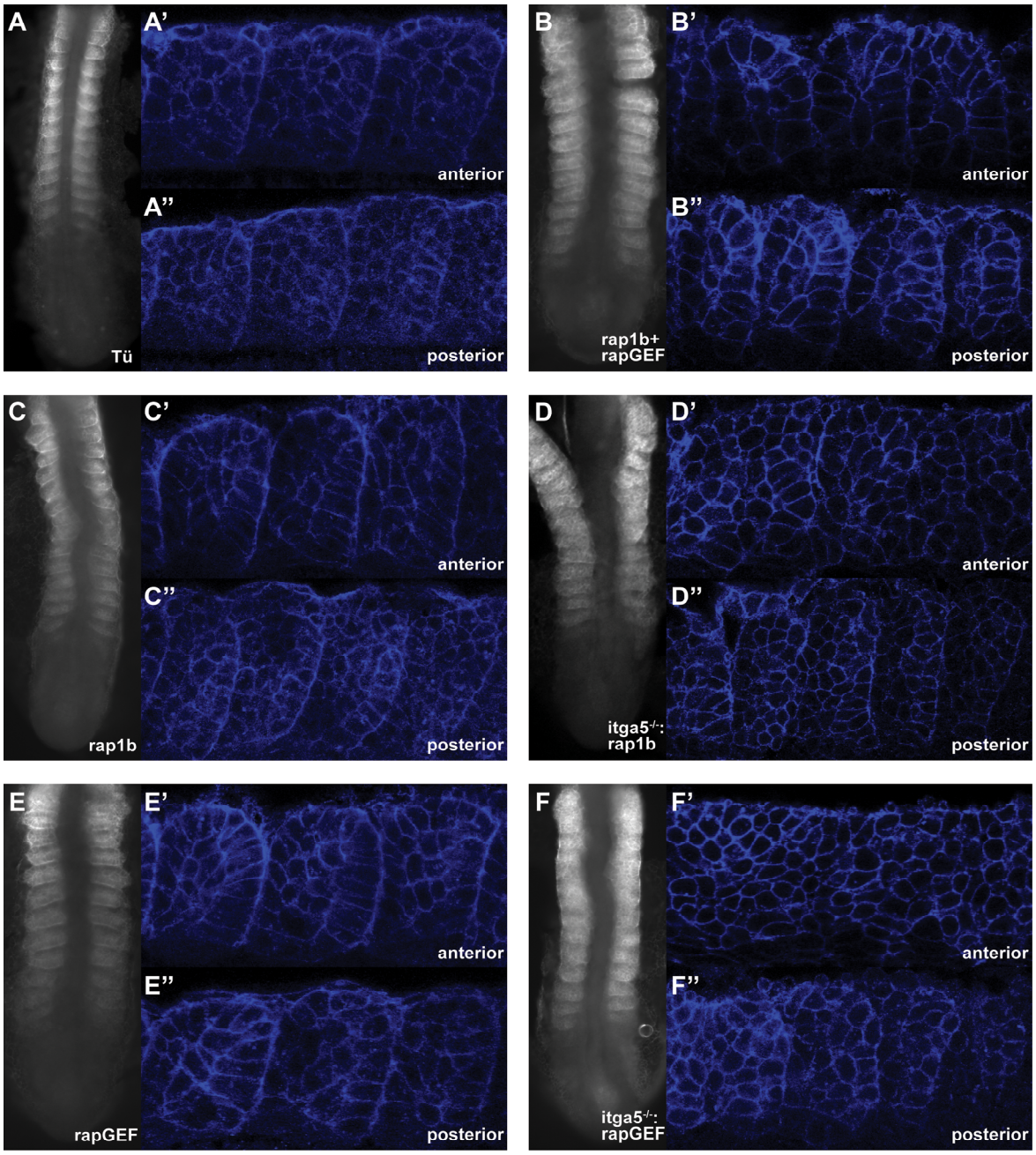

Figure 12. Segment polarity in mature somites

ephrinB2a (white, blue) immunostaining of embryos at 12-15 somite stage (A-F). Confocal image of the most anterior somites (A'-F') and the most posterior somites (A''-F''). *ephrinB2a* is expressed in the posterior half of each somite. Wild-type embryo (A). Knockdown of *rap1b* (C, C',C''), *rapGEF* (E,E',E'') and *rap1b* together with *rapGEF* (B, B',B'') showed only minor defects on the expression pattern, whereas knockdown of *rap1b* (D,D',D'') and *rapGEF* (F,F',F'') in *bfe/integrinα5* mutant embryos led to modest defects in the anterior expression pattern.

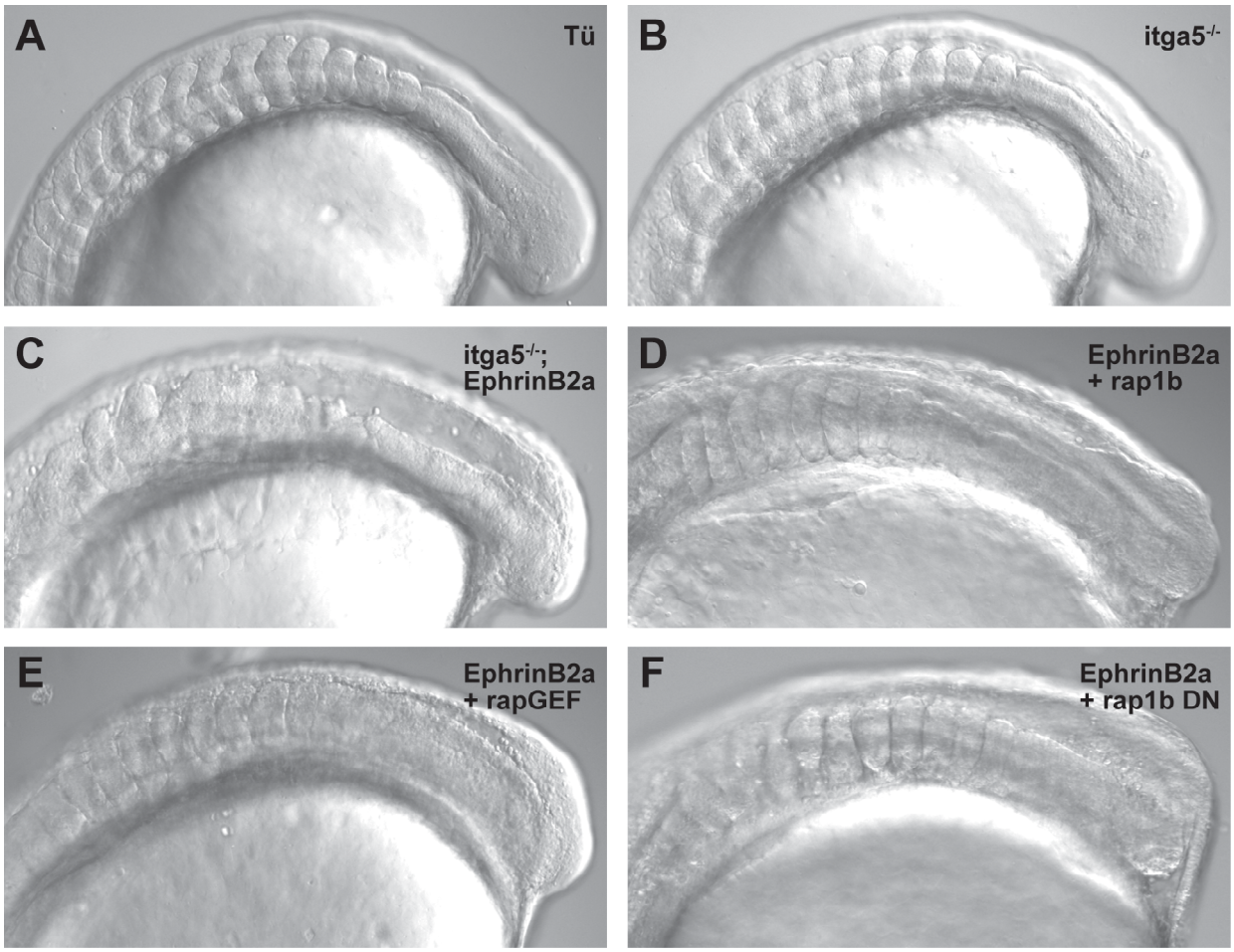

Figure 13. Inhibition of *ephrinB2a* function in combination with *rap1b* and *rapGEF* function

Wild-type embryo (A) and *bfe/integrinα5* mutant embryo (B) at 12-15 somite stage. Morpholino-mediated knockdown of *ephrinB2a* (C) in *bfe/integrinα5* mutant embryos led to fused somite phenotype. Knockdown of *rap1b* (D) and *rapGEF* (E) in combination with *ephrinB2a* led to strong anterior-posterior axis extension defects, so did injection of dnRap1b(S17N) mRNA together with *ephrinB2a* morpholino (F).

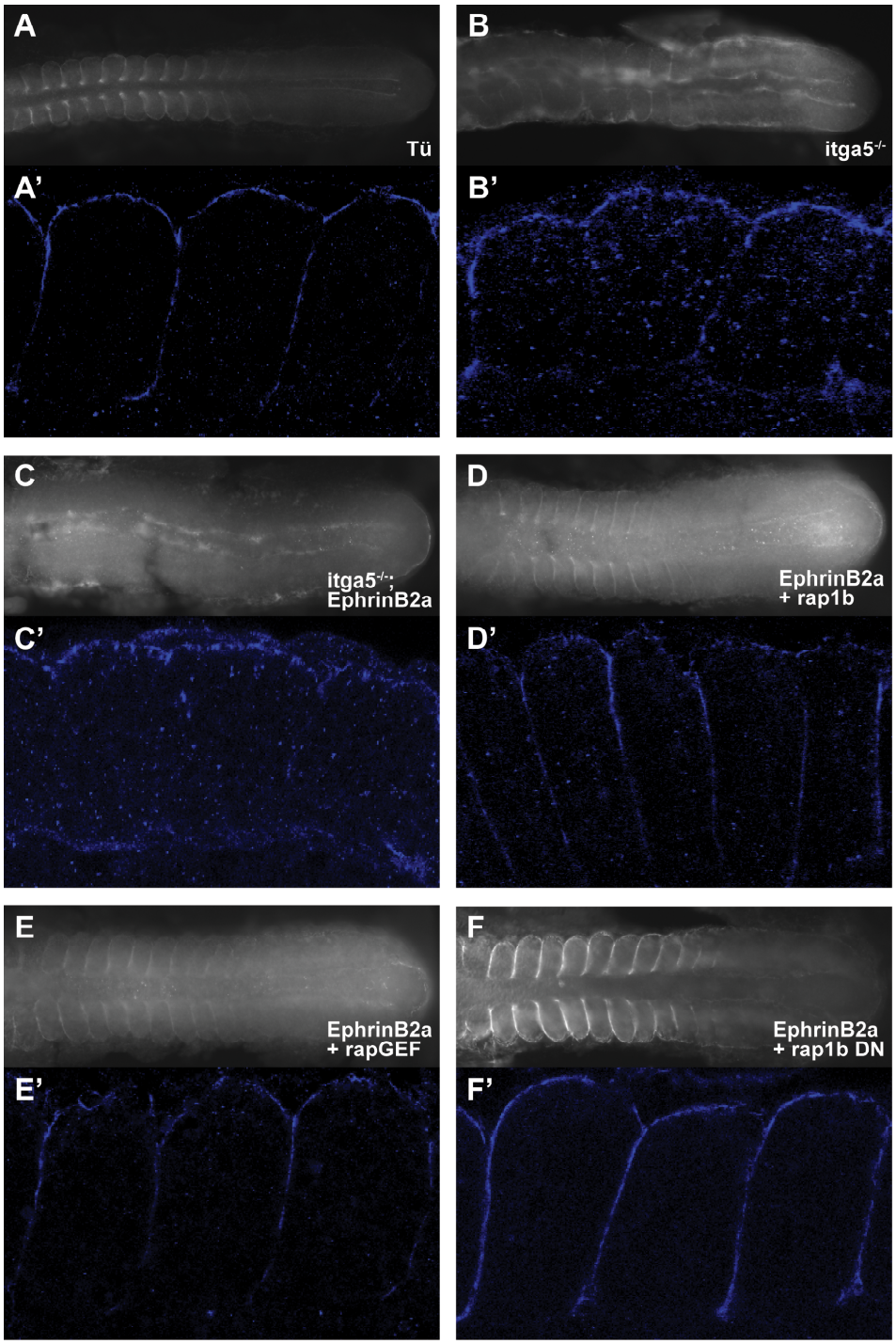

Figure 14. Fibronectin matrix assembly

Fibronectin (white, blue) immunostain of embryos at 12-15 somite stage (A-F). Confocal images of the most posterior somites (A'-F'). Wild-type embryo (A, A'). *bfe/integrinα5* mutant embryo (B, B'). Knockdown of *ephrinB2a* (C, C') in *bfe/integrinα5* mutant embryos led to almost complete loss of Fibronectin matrix assembly. Double knockdown of *ephrinB2a* together with *rap1b* (D, D') or *rapGEF* (E, E') led to minor defects in Fibronectin matrix assembly, so did *ephrinB2a* in combination with injection of dnRap1b(S17N) (F, F').

3. Discussion

3.1. Rap1a, Rap1b and RapGEF are involved in convergent extension movements during zebrafish development

The main function of the small GTPase Rap1 during zebrafish development was largely unknown. Therefore, it was of interest to first characterize the function of *rap1a*, *rap1b* and a *rapGEF* in general. Knockdown of *rap1a*, *rap1b* and *rapGEF* in wild-type embryos generated, in all three assays, a defect in axis extension and tail elongation, which is consistent with previous studies (Tsai et al. 2007). The similarity in phenotype of all three morphants suggests that they are involved in the same developmental process (Table 1). Double knockdown of *rap1b* and *rapGEF* generated an enhancement of both phenotypes, which emphasises that *rap1b* and *rapGEF* may function together during axis extension and tail elongation. The generation of a dominant-negative Rap1b (dnRap1b) enabled to circumvent genetic redundancy. dnRap1b has a point mutation at the GTP binding site and cannot bind GTP anymore, thereby mimicking the inactive GDP bound state. Injection of the dnRap1b construct into wild-type embryos generated, similar to knockdown of *rap1b* and *rapGEF*, a defect in axis extension and tail elongation. Furthermore, combinations with either *rap1b* or *rapGEF* morpholino led to an enhancement of the single morphants phenotypes similar to the double knockdown of *rap1b* and *rapGEF*. These results emphasised that both *rap1b* and *rapGEF* might function together during convergence extension movements and tail elongation. Interestingly, embryos lacking the proper function of either *rap1b* or *rapGEF* or both, exhibited very significant tail phenotypes, characterized by an aggregation of cells at the dorsal side of the tail bud. This tail phenotype was significantly enhanced in the dnRap1b combinations, where on first glance it seemed that the epidermis of the embryo detached from the underlying tissue. It appeared that the epidermal morphogenesis defect did not allow tail extension, and that therefore cells of the tail bud are forced to move dorsally above the tail bud instead of extending the tail posteriorly, generating the visible empty space dorsally above the posterior somites. Nevertheless, analysis of *rap1b* and *rapGEF* function in wild-type embryos did not assign any specific function during the process of somitogenesis. The embryos exhibited a temporal delay in somite formation, but did not show any defects in the

segmentation itself. The morphants exhibited minor differences in somite size and shape compared to wild-type embryos, which might be due to the convergent-extension defect.

3.2. Rap1b and RapGEF interact with Integrinα5 during somite border morphogenesis

Inhibition of *rap1b* or *rapGEF* function in wild-type embryos did not exhibit a segmentation defect, whereas knockdown of *rap1b* or *rapGEF* in *bfe/integrinα5* mutant embryos led to a strong enhancement of the segmentation defect. *bfe/integrinα5* embryos exhibit aberrant anterior somite border maintenance, which was enhanced by inhibition of *rap1b* or *rapGEF* function in that even posterior somite border formation was affected. Additionally, defects in axis extension and tail elongation were enhanced. These phenotypes revealed a genetic interaction between Integrinα5 and the Rap1 signalling in both axis elongation and somite morphogenesis (Table 1). The observed synergy between knockdown of either *rap1b* or *rapGEF* in *bfe/integrinα5* mutant embryos suggests that these genes function in regulating cell migration and extracellular matrix assembly. Specifically, the loss of Fibronectin matrix assembly in the *rap1* morpholino-mediated knockdowns in *bfe/integrinα5* mutant embryos suggested that Rap1 might be involved in the Integrinα5 'inside-out' signalling.

The modest impact on the segmental expression patterns of the clock gene *her-1*, of the segment marker *myo-D* and the segment polarity markers *ripply-1*, *mesp-b* and *ephA4* suggested that the small GTPase Rap1 and Integrinα5 do not have important functions in the establishment of the segmental pattern or segment polarity. It rather seemed that they are primarily involved in converting this patterning information into morphological segmentation.

3.3. EphrinB2a interacts with Integrinα5 during somite morphogenesis

Studies have shown that Integrin-Fibronectin interaction and Eph/Ephrin signalling function together during somite morphogenesis (Barrios et al. 2003, unpublished data). Additionally, studies implicated a role for the Rap1 GTPase in processes involving Eph/Ephrin signalling in cell culture and Integrin signalling in the immunesysteme. However, a genetic interaction between Raps and Eph/Ephrin signalling or Integrin signalling during somite border formation was so far not shown yet.

Although knockdown of *ephrinB2a* in wild-type embryos (Koshida et al. 2005) did not generate, like *rap* morphants any somite border defects, knockdown of *ephrinB2a* in *bfe/Integrinα5* mutant embryos generated fused somites (van Eeden et al. 1996). Somite borders were initially formed but not maintained and embryos exhibited a complete loss of Fibronectin matrix assembly throughout the paraxial mesoderm. These observations confirmed a genetic correlation between EphrinB2a and Integrinα5 during somite border formation (Table 1).

3.4. EphrinB2a interacts with Rap1b and RapGEF during convergent extension movements

To look for genetic interaction between EphrinB2a and the Rap1 GTPase, loss-of-function experiments were performed. However, inhibition of *rap1b* and *rapGEF* function in combination with knockdown of *ephrinB2a* in wild-type embryos produced unexpected no obvious somite border defect. The morphants did exhibit very strong defects in axis extension and tail elongation (Table 1). Fibronectin matrix assembly appeared normal, although the staining was slightly weaker compared to wild-type embryos.

Phenotype ➔ Genotype ⬇	Axis extension defect	Tail elongation defect	Somite border defect	Fibronectin assembly defect
rap1b	+	+	-	-
rapGEF	+	+	-	-
dnRap1b	+	+	-	-
rap1b + *rapGEF*	+ +	+ +	-	-
rap1b + dnRap1b	+ +	+ +	-	-
rapGEF + dnRap1b	+ +	+ +	-	-
itga5$^{-/-}$	-	-	+	+
rap1b; itga5$^{-/-}$	+ +	+ +	+ +	+ + +
rapGEF; itga5$^{-/-}$	+ +	+ +	+ +	+ + +
dnRap1b*; itga5*$^{-/-}$	+ +	+ +	+ +	+ + +
ephrinB2a; itga5$^{-/-}$	+ +	+ +	+ + +	+ + +
rap1b + *ephrinB2a*	+ + +	+ +	-	-
rapGEF + *ephrinB2a*	+ + +	+ +	-	-
rapGEF + *ephrinB2a*	+ + +	+ +	-	-

Table 1

Summery of loss-of-function phenotypes with defects in axis elongation, tail elongation, somite border formation and Fibronectin matrix assembly. (-) no defect, (+) mild defect, (++) enhanced defect, (+++) more severe defect

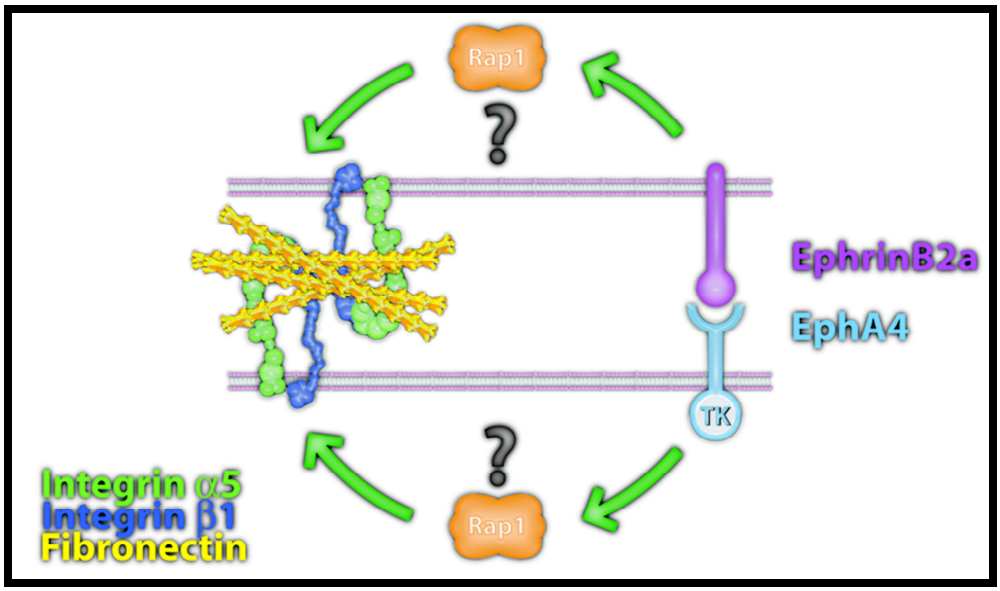

Figure 1. Hypothesised signalling pathway

Eph/Ephrin signalling activates the small GTPas Rap1 either via EphA4 ‘forward’ or EphrinB2a ’reverse’ signalling. In turn, the small GTPase Rap1 causes Integrinα5 clustering and therefore mediates via ‘inside-out’ signalling and Fibronectin matrix assembly.
Figure 1 was provided with permission by Scott Holley.

3.5. Conclusion and Future Objectives

In conclusion, loss-of-function experiments showed a genetic interaction between Integrinα5 and the Rap1 GTPase, between EphrinB2a and the Rap1 GTPase and between Integrinα5 and EphrinB2a. Given that inhibition of *rap1b* and *rapGEF* function in wild-type embryos led to axis extension defects and tail elongation defect, the small GTPase Rap1 appeared to be involved in cell migration during convergence extension movements and tail elongation. Furthermore, the enhancement of the *rap1b* and *rapGEF* loss-of-function phenotype via *ephrinB2a* knockdown suggests that EphrinB2a and the GTPase Rap1 function either directly or indirectly in a signalling pathway controlling axis extension and tail elongation during zebrafish development. Inhibition of *rap1b* and *rapGEF* function in *bfe/integrinα5* mutant embryos created a strongly enhanced somite border defect, similar to the phenotype observed in *ephrinB2a* knockdown in *bfe/integrinα5* mutant embryos. This strong enhancement of the phenotype of the *bfe/integrinα5* mutant suggests, that both EphrinB2a and the small GTPase Rap1 are interacting with the Integrinα5 during somite border morphogenesis. The loss of Fibronectin matrix assembly in these morphants supports the hypothesis that Integrin-Fibronectin interaction is regulated via 'inside-out' signalling, directly or indirectly via EphrinB2a and/or the Rap1 GTPase.

To investigate the direct or indirect link between EphrinB2a, rap1b, rapGEF and Integrinα5, the study could be continued by generating genetic mosaics via cell transplantation to perform epistasis experiments. Genetic mosaics could examine whether the Rap1 GTPase is necessary for Eph/Ephrin-dependent Integrinα5 clustering and Fibronectin matrix formation (Figure 1). Furthermore, it would be interesting to examine whether Rap1 GTPase functions in either forward or reverse Eph/Ephrin signalling (Figure 1) as the literature contains conflicting reports of the relationship between these signalling pathways.

4. Materials and Methods

4.1. Isolation of total RNA

Total RNA was prepared from 12-15 somite stage embryos using RNAwiz™ RNA Isolation Reagent (Ambion). 250µl RNAwiz was added to about 50 embryos in a 1.5ml eppendorf tube. Embryos were then immediately homogenized using a pestle. After the homogenate was incubated for 5 minutes at RT, 50µl Chloroform was added, vigorously shaken for 15 seconds and incubated for 10 minutes at RT. To separate phases, homogenate was centrifuged for 15 minutes at 5000 rpm at 4°C, the colourless upper phase was transferred to a fresh tube without disturbing the interphase and 125µl ddH_2O was added and vortexed. 250µl isopropanol was added, vortexed and incubated at RT for 10 minutes, centrifuged at 5000 rpm for 15 minutes at 4°C. The pellet was washed with 75% ice-cold ethanol and centrifuged for 5 minutes at 5000 rpm at 4°C. The wash was repeated, the pellet was air dried and resuspended in 12µl RNase-free ddH_2O. The concentration and purity of the sample was checked using a spectrophotometer.

4.2. First-strand cDNA synthesis

SuperScript™ II Reverse Transcriptase (Invitrogen) was used to perform the first-strand cDNA synthesis. Ideally, 5µg (or as much as possible to a final volume of 11µl) of total RNA, 1µl 10µM Oligo dT and H_2O to a final volume of 11µl were incubated at 70°C for 10 minutes. The reaction mix was immediately cooled on ice before adding 5x PCR Buffer, 10mM dNTP mix, 100mM DTT and 1 µl SupersScript™ II RT. The reaction was incubated at 42°C for 1 hour and at 70°C for 15 minutes, then placed on ice. To remove RNA, 1µl of RNase H (Roche) was added and incubated for 20 minutes at 37°C. cDNA was stored at -80°C.

4.3. RACE cDNA amplification

A full-length clone of the zebrafish rapGEF gene was obtained by 5' rapid amplification of cDNA ends (RACE) using SMART^{TM} RACE cDNA Amplification Kit (Clontech). During first-strand cDNA synthesis, a specific primer (SMART II A oligo) is used to add the SMART sequence tag at the 5'end. In subsequent PCR, a universal primer mix (UPM) that recognizes the SMART sequence is used in conjunction with a gene specific primer (rapGEF 5'GSP1) to amplify the 5' end of the target cDNA. Specific fragments are then amplified further by PCR using nested primers. Total RNA was prepared from 12-15 somite stage embryos as described in section 2.1. For the first-strand cDNA synthesis, 1µg of total RNA was mixed with 1µl 5'-RACE CDS primer A, 1µl SMART II A oligo and H_2O to a final volume of 5µl. Reactions were incubated for 2 minutes at 70°C, cooled down for 2 minutes on ice and spun down briefly before adding the following: 2µl 5x First-Strand buffer, 1µl 20mM DTT, 1µl 10mM dNTP mix and 1µl MMLV (Murine Leukemia Virus) Reverse Transcriptase to a final volume of 10µl. Reactions were mixed by gently pipetting and spun down before incubating at 42°C for 1.5 hours in a hot-lid thermal cycler. The reaction product was diluted with 100µl Tricine-EDTA buffer and heated at 72°C for 7 minutes. The 5' RACE-Ready cDNA was stored at -20°C. For the actual 5'RACE, PCR was performed using Phusion high fidelity (HF) DNA polymerase (Finnzymes). Individual reactions contained 10µl 5x Phusion HF buffer, 1µl 10mM dNTP mix, 0.5µl Phusion DNA Polymerase, 2.5µl of 5' RACE-Ready cDNA, 5µl 10x UPM (Universal Primer Mix), 1µl 10µM rapGEF 5'GSP1 and H_2O to a final volume of 50µl was prepared and were subjected to the following running conditions using an iCycler^{TM} Thermal Cycler (Biorad): 5 cycles of 30s at 94°C, 60s at 72°C, 5 cycles of 30s at 94°C, 30s at 70°C, 60s at 72°C and 25 cycles of 30s at 94°C, 30s at 65.6°C, 60s at 72°C. 5µl of the primary PCR-product was diluted in 245µl of Tricine-EDTA buffer and a 'nested' PCR was performed using an internal, nested primer (rapGEF 5'NGSP1) predicted to anneal ~75bp upstream of the rapGEF 5'GSP1 sequence was performed. A reaction mix consisting of 5µl of the diluted primary PCR product, 1µl 10µM NUP (Nested Universal Primer), 1µl 10µM rapGEF 5'NGSP1, 10µl 5x Phusion HF buffer, 1µl 10mM dNTP mix, 0.5µl Phusion HF DNA Polymerase (Finnzymes) and H_2O to a final volume of 50µl was prepared and subjected to the following running conditions: 20 cycles of 30s at 94°C, 30s at 65.6°C and 60s at 72°C. The PCR product was run on a 2% agarose gel containing 0.01% ethidium bromide, showing several bands of sizes from 50bp to 500bp.

DNA fragments at size between 400 and 500bp were excised and DNA purification was performed using Zymoclean Gel DNA Recovery Kit™ (Zymo Research) as described in section 2.4.2. RACE products were characterized by sequencing (described in section 2.4.6.) and aligning (using DNAstar software) with the existing incomplete rapGEF sequence obtained from the Wellcome Trust Sanger Institute (http://www.sanger.ac.uk). 5' RACE-Ready cDNA was used to amplify the complete rapGEF coding sequence with the new predicted start-codon, which was then cloned into the pCS2+ vector for further analysis.

4.4. Molecular Cloning

4.4.1. PCR amplification

Phusion high fidelity DNA polymerase (Finnzymes) was used to amplify DNA fragments from plasmid or cDNA templates for cloning. Reaction mixtures comprised 5µl Phusion HF Buffer, 10mM dNTPs, 0.5µM forward and reverse primer, 0.1µl template DNA, 0.02U/µl Phusion DNA polymerase and H_2O to a final volume of 25µl and were subjected to the following general running conditions using iCycler™ Thermal Cycler (Biorad): 30s at 98°C, 35 cycles of 10s at 98°C, 15s at primer annealing temperature, 15s/1kb template at 72°C and 7 minutes at 72°C.

4.4.2. DNA purification

PCR products were run on a 1% agarose gel containing 0.01% ethidium bromide for about 40 minutes at 100 Volts. DNA fragments of interest were excised using a scalpel and purified using the Zymoclean Gel DNA Recovery Kit™ (Zymo Research). Following the manufacturers instructions, 3 volumes of ADB Buffer™ were added per volume of gel and incubated at 55°C until the gel was completely dissolved. The solution was transferred to a Zymo-Spin I™ Column, centrifuged at maximum speed for 30 seconds and the flow-through was discarded. 200µl Wash Buffer was added and centrifuged at maximum speed for 30 seconds. The flow-through was discarded and the wash was repeated. To elute the DNA 6-13µl of ddH_20 was applied directly to the column matrix and centrifuged for 1 minute.

4.4.3. Restriction digest and ligation

All inserts were cloned into the pCS2^{+} vector (Rupp et al. 1994, Turner and Weintraub 1994): 1µg DNA, 5µl of the appropriate 10x buffer (NEB), 0.5µl of 100x BSA (if required), 10-20 units restriction enzyme (NEB) and H_20 to a final volume of 50µl and were incubated at 37°C for 3 hours or overnight. To circumvent re-ligation of vector, the linearised DNA was dephosphorylated by incubating with 0.5µl of Calf Intestinal Alkaline Phosphatase (NEB) for 50 minutes at 37°C. DNA concentrations were estimated from agarose gels. Ligation reactions contained insert and vector DNA were added at a 3:1 molar ratio with 1µl 10x NEB T4 Ligase Buffer, 0.5µl T4 DNA Ligase and H_2O to a final volume of 10µl. Ligations were incubated overnight at 16°C.

4.4.4. Transformation

Electrocompetent *E.coli* (DH5α) cells were gently defrosted on ice. 1µl of the ligation was added to 40µl DH5α cells and transferred to a pre-chilled Gene Pulser® Cuvette (Biorad) with 0.1cm electrode gap. The cells were electroporated using a Micropulser^{TM} (Biorad), 1ml of 37°C pre-warmed SOC media was immediately added and cells were incubated at 37°C for 1 hour shaking at 300rpm. Transformed cells were plated on LB amp+ plates and incubated overnight at 37°C.

4.4.5. Plasmid DNA purification

4.4.5.1.Plasmid Miniprep

Plasmid DNA was prepared from transformed bacteria by standard alkaline lysis (Sambrook and Russell 2001). Single colonies were picked, inoculated into 2ml Luria-Bertani (LB) containing 50mg/ml Ampicillin (amp+) and incubated overnight at 37°C shaking at 300rpm. 1.5ml of the culture was harvested by centrifugation at maximum speed for 30 seconds at 4°C. The bacterial pellet was resuspended in 100µl of ice-cold Alkaline lysis solution I (50mM glucose, 25mM Tris-Cl pH 8.0 and 10mM EDTA pH 8.0), 200µl freshly prepared Alkaline lysis solution II (0.2 N NaOH, 1%(w/v) SDS) was added and mixed by rapidly inverting the tube several times. 150µl ice-cold Alkaline lysis solution III (3M potassium

acetate, 11.5% glacial acetic acid) was added and contents was mixed by inverting the tube several times. Tubes were placed on ice for 5 minutes, then centrifuged at maximum speed for 10 minutes at 4°C. The supernatant was transferred to a fresh tube and 2 volumes of isopropanol was added. The solution was vortexed, incubated for 2 minutes at RT and centrifuged at maximum speed for 20 minutes at 4°C. The liquid was removed, 1ml of 70% ethanol was added to the pellet, centrifuged at maximum speed for 2 minutes at 4°C and supernatant was discarded. The pellet was air-dried, dissolved in 50µl TE pH 8.0 containing 20µg/ml DNase-free RNase A (Roche) and stored at -20°C.

4.4.5.2. Plasmid Midiprep

Larger scale preparations of plasmid DNA were performed with the Qiafilter Plasmid Midi Kit (Qiagen), according to the manufacturers protocol. Single colonies were picked, inoculated into 2ml LB amp+ and incubated overnight at 37°C shaking at 300rpm. The starter culture was diluted 1:1000 in LB amp+ (50mg/ml) medium and incubated overnight at 37°C shaking at 300rpm. The cells were harvested by centrifugation at 600xg for 15 minutes at 4°C and the pellet was resuspended in 4ml Buffer P1. 4ml Buffer P2 was added and tube was vigorously inverted several times and incubated at RT for 5 minutes. 4ml chilled Buffer P3 was added immediately and mixed by inverting the tube. The lysate was poured into the barrel of a QIAfilter cartridge and incubated for 10 minutes at RT. In the meantime, a QIAGEN-tip 100 column was equilibrated with 4 ml Buffer QBT. The lysate was filtered through the cartridge into the column and allowed to enter the resin by gravity flow. The column was washed twice with 10ml Buffer QC and the DNA was eluted in 5ml Buffer QF. 3.5ml isopropanol was added to the eluted DNA, mixed and centrifuged at 15000xg for 30 minutes at 4°C. The supernatant was discarded and the pellet was washed with 2ml 70% ethanol, centrifuged at 15000xg for 10 minutes. The supernatant was discarded, the pellet air-dried and the DNA was redissolved in 250µl TE pH 8.0.

4.4.6. Sequencing

Samples for sequencing were sent to W.M Keck Foundation Biotechnology Resource Laboratory (Yale School of Medicine) according to their guidelines: 500-600ng plasmid DNA template and 2µl 4µM primer were mixed with H_2O to a final volume of 18µl. For PCR

products, 10-20ng template per every 200 bases of fragment was mixed with 2µl 4µM primer and H_2O to a final volume of 18µl.

4.5. *in vitro* transcription

Linearized DNA templates for mRNA (Table 1) and riboprobe (Table 2) synthesis were prepared by restriction digest of plasmids as described in section 2.4.3. To clean the template, 1 µl (20µg/µl) Proteinase K and 0.75µl 20% SDS were added and incubated for 45 minutes at 65°C. The entire reaction was run on an agarose gel and the template fragment was excised and recovered using Zymoclean™ Gel DNA Recovery Kit (Zymo Research), as described in section 2.4.2.

4.5.1. mRNA synthesis

in vitro transcription was performed using the mMessage mMachine High yield capped RNA Transcription Sp6 Kit (Ambion), following the manufacturers protocol. Reactions containing 10 µl 2xNTP/CAP, 2µl 10x reaction buffer, 6µl (1µg) linear DNA template and 2 µl Sp6 enzyme mix were incubated for 2 hours at 37°C. To remove the template, 1µl of TURBO DNase was added and incubated for additional 15 minutes at 37°C. The RNA was purified using Micro Bio-Spin Columns (P-30 Tris RNase-free, Biorad), according to the manufacturers instructions. The columns were equilibrated by allowing the excess packing buffer to drain by gravity-flow for about 2 minutes and subsequently centrifuged at 1000xg for 2 minutes to remove remaining packing buffer. The sample was applied directly onto the gel bed and centrifuged for 4 minutes at 1000xg. After this procedure the purified sample was in 10mM Tris buffer and stored at -80°C.

mRNA	Template	Linerized with
Rap1b	pCS2+/rap1b	NotI
Rap1b-GFP	pCS2+/rap1b-GFP	NotI
Rap1b-(S17N)-DN	pCS2+/rap1b-(S17N)-DN	NotI
RapGEF	pCS2+/rapGEF	XbaI
rapGEF-GFP	pCS2+/rapGEF-GFP	XbaI

Table 1

mRNAs for microinjection generated from a linearised vector as a template

4.5.2. Riboprobe synthesis

Reactions containing 13µl (1µg) linearised plasmid DNA, 2µl 10x RNA polymerase buffer (NEB), 2µl 10x Digoxigenin (DIG) or Fluorescein RNA labelling mix (Roche), 1µl RNase inhibitor (Roche) and 2µl T7 RNA Polymerase (NEB) were incubated for 2 hours at 37°C. To remove the template, 1µl RNase-free DNase (Roche) was added and incubated for additional 15 minutes at 37°C. The RNA was purified using Micro Bio-Spin Columns (P-30 Tris RNase-free, Bio-Rad), as described in section 2.5.1. and 19µl formamide was added to the eluate and riboprobes were stored at -20°C.

Riboprobe	Template
her-1	provided by Scott Holley
myo-D	provided by Scott Holley
ripply-1	provided by Lixia Zhang
ephA4	provided by Steve Wilson (UCL)
Rap1b	pCS2+/rap1b

Table 2

Riboprobes for *in situ* hybridisation assay generated from a linearised vector as a template

The template for the Riboprobe rapGEF was generated via PCR as described in section 2.4.1 and 13µl of PCR product was used for above described Riboprobe synthesis reaction.

Riboprobe	Vector	Primer
rapGEF antisense	pCS2+/rapGEF	rapGEF new 5' rapGEF T7

Table 3

Riboprobe for *in situ* hybridisation produced from a template generated by PCR

4.6. Primer sequences

rapGEF 5'GSP1	GCCCTCATCCACCAAAACCTGCCACATTC	2.3.
rapGEF 5'NGSP1	CCAATCCACAAGCTCCTTTCCGCTGCAGC	2.3.
5.Rap1a EcoRI	CGGAATTCATGCGTGAATATAAGCTTGTG	2.4.
3.Rap1a XhoI	CGTTGGCTCGAGTTACAGCAGGACACAGTTTGAC	2.4.
rap1b 5'EcoRI	CGAATTCATGCGTGAATACAAGTTAGTA	2.4.
rap1b 3'XbaI	GTTCTAGATTAGAGCAACTGGCAGGTGGACT	2.4.
emGFP BamHI F	CAGGATCCATGGTGTCCAAGGGCGA	2.4.
emGFP EcoRI R	GGAATTCCTTGTACAGCTCGTCCAT	2.4.
rap1b N17 F	GGTGTTGGCAAGAATGCGCTGACTGTT	2.4.
rap1b N17 R	AACAGTCAGCGCATTCTTGCCAACACC	2.4.
rap1b HindIII 1F	GGAGCAAGCTTGATTTAGGTGA	2.4.
emGFP ClaI R	GCATCGATCTTGTACAGCTCGTCCA	2.4.
emGFP ClaI F	ATATCGATATGGTGTCCAAGGGCGA	2.4.
rapGEF new 5'	ATGCATCTCTTTCGGAGTTAC	2.5.2.
rapGEF T7	GTAATACGACTCACTATAGGGCCTGAGTTAGTTTCTTCTGATTGTC	2.4.2.

Table 4

Primer sequences given in 5' to 3' direction

4.7. *in situ* hybridisation

Embryos were fixed in 4% paraformaldehyde (PFA) in PBS (0.8% NaCl, 0.02% KCl, 0.02 M PO4 pH 7.3) overnight at 4°C, washed and dechorionated in PBST (0.1% Tween in PBS), then processed through a series of washes in 25%, 50%, 75% methanol in PBST and 100% methanol for 5 minutes each. Embryos were transferred to fresh 100% methanol and stored at -20°C for one hour or overnight. Embryos were re-hydrated by performing the reciprocal methanol series and washed twice with PBST for 5 minutes at room temperature (RT). Incubation in Proteinase K (5µg/ml in PBST)(Roche) was performed for 1-3 minutes, depending on the age of the embryos. Embryos were immediately washed twice for 5 min with PBST, fixed with 4% PFA/PBS for 20 minutes at RT, washed twice again and incubated in 100µl HYB^- (50% Formamide, 5x SSC, 0.1% Tween-20) for 5 minutes at 65°C. Pre-

hybridisation for 1 hour at 65°C was performed by adding 50µl pre-warmed HYB^+ (HYB^-, 5mg/ml torula (yeast) RNA, 50µg/ml heparin). For the hybridisation, HYB^+ was replaced with fresh 30µl fresh HYB^+ including appropriate riboprobes and embryos were incubated at 65°C overnight. The probe was removed and embryos were washed at 65°C: twice for 30 minutes with freshly prepared 50% Formamide/2xSCCT (0.1% Tween in SSC), once for 15 minutes with 2xSSCT and twice for 30 minutes with 0.2xSSCT. Embryos were blocked for at least 1 hour at RT with 2% Blocking reagent in 1x maleic acid buffer (150mM maleic acid, 100mM NaCl pH 7.5), then incubated overnight at 4°C in anti-DIG (Digoxigenin) Fab-AP (Alkaline Phosphatase) (Roche) diluted 1:5000 in 2% Blocking reagent (Roche) in 1x maleic acid buffer. Embryos were washed four times for 20 minutes in 1x maleic acid buffer and three times for 5 minutes in NBT/bCIP staining buffer (100mM Tris pH 9.5, 100mM NaCl, 50mM MgCl2, 0.1% Tween-20). To detect the DIG-labelled probe, embryos were incubated in the dark in NBT/bCIP staining buffer containing 4.5µl NBT (NBT:75mg/ml in 70% dimethylformamide) and 3.5µl bCIP (X-Phosphate: 50mg/ml in dimethylformamide) per ml. Once a satisfactory level of staining was achieved, embryos were washed three times in PBST, fixed for 20 minutes in 4%PFA/PBS and washed again twice for 5 minutes in PBST. A methanol series was performed and embryos were incubated in fresh 100% Methanol for 30 minutes at RT or overnight at 4°C. Embryos were re-hydrated performing the reciprocal methanol series and washed twice with PBST for 5 minutes at RT. Embryos processed through series of 25%, 50% and 75% glycerol in PBST and stored overnight at 4°C in 75% glycerol in PBST.

For double *in situ* hybridisation, embryos were after 20 minutes 4%PFA/PBS fixation and two 5 minutes PBST washes, incubated twice for 15 minutes in 100mM glycine pH 2.2 and washed twice for 5 minutes in PBST. A methanol series was performed and embryos were incubated in fresh 100% Methanol for 30 minutes at RT or overnight at 4°C. Embryos were re-hydrated performing the reciprocal methanol series and washed twice with PBST for 5 minutes at RT. Prior to detection of the Fluorescein-labelled probe, embryos were blocked again for at least 1 hour at RT with 2% Blocking reagent in 1x maleic acid buffer, then incubated overnight at 4°C in anti-Fluorescein Fab-AP (Roche) diluted 1:500 in 2% Blocking reagent in 1x maleic acid buffer. Embryos were washed four times for 20 minutes in 1x maleic acid buffer and three times for 5 minutes in Fast-Red staining buffer (100mM Tris pH 8.2, 100mM NaCl, 50mM $MgCl_2$, 0.1% Tween-20). To stain embryos, one Fast-Red tablet (Roche) was dissolved in 4 ml Fast-Red staining buffer, 50mg/ml NAMP (Naphtol AS-MX Phosphate) in DMSO was diluted 1:100 in Fast-Red staining buffer, and both reagents were

mixed 1:1 before adding to the embryos. After staining, embryos were washed in PBST, fixed for 20 minutes in 4% PFA/PBS and washed twice for 5 minutes in PBST. Embryos processed through series of 25%, 50% and 75% glycerol in PBST and stored overnight at 4°C in 75% glycerol in PBST. Embryos were deyolked, dissected and flat mounted in 75% glycerol in PBST.

4.8. Fibronectin or EphrinB2a antibody stain

Embryos were fixed in 4% paraformaldehyde (PFA) in PBS (0.8% NaCl, 0.02% KCl, 0.02 M PO4 pH 7.3) overnight at 4°C, washed and dechorionated in PBSDT (1%DMSO, 0.1% Triton X-100 in PBS) and washed twice for 5 min. Embryos were treated with Proteinase K (5µg/ml in PBSDT) for 1-3 minutes, depending on the developmental stage. Embryos were immediately washed twice for 5 minutes with PBSDT, fixed with 4% PFA/PBS for 20 minutes at RT, washed twice again, then blocked for at least 1 hour at RT in 1% Blocking reagent (Roche) in PBSDT. Primary antibody incubations were performed overnight at 4C. Specific antibodies used were: rabbit anti-human Fibronectin IgG (Sigma) diluted 1:100 in 1% blocking reagent in PBSDT; goat anti-ZF EphrinB2a (Research&Development systems) diluted 1:1000 in 1% blocking reagent in PBSDT. After washing four times with PBSDT for 15 minutes, embryos were incubated overnight at 4°C with the appropriate secondary antibody. For Fibronectin: Alexa Fluor 488 donkey anti-rabbit IgG (Molecular Probes) diluted 1:200 in 1% Block in PBSDT. For EphrinB2a: Alex Fluor 488 rabbit anti-goat (Molecular Probes) diluted 1:200 in 1% Block in PBSDT. Embryos were washed three times for 10 minutes in PBSDT, fixed for 20 minutes in 4% PFA/PBS at RT and washed twice for 5 minutes in PBST. To store embryos at 4°C, a glycerol series of 7 minutes each in 25%, 50%, 75% glycerol in PBST was performed.

4.9. Zebrafish strains

To characterize the function of rapGTPase *rap1a* and *rap1b* and the *rapGEF*, the wild-type Tübingen strain was used. Synergetic effects between *rap* genes or *ephrinB2a* and *integrinα5* were investigated using fish carrying the *integrinα5* mutant alleles bfe^{th30} or bfe^{tig453}.

Fish were raised and maintained using a recirculation water system (Brand et al., 2002).

4.10. Microinjection

Morpholinos or mRNA were injected into 1-cell stage embryos as described previously (Nüsslein-Volhard and Dahm 2002). mRNA was generated by *in vitro* transcription, as described in section 2.5.1. Morpholinos were synthesised by Gene Tools and diluted in 1x Danieau solution (58mM NaCl, 0.7mM KCl, 0.4mM MgSO4, 0.6mM Ca(NO3), 2,5mM HEPES, pH 7.6). The translation-blocking morpholino against *rapGEF* was designed to bind the 5'UTR (un-translated region) upstream of the translation initiation codon, whereas the splice-blocking morpholino was designed to bind the junction of the first exon and first intron. The morpholinos targeting *rap1b* ad *ephrinb2a* have been described previously (Koshida et al. 2005, Tsai et al. 2007).

Morpholino	Sequence	Binding Side	Conc.
***rap1a* (Tsai et al. 2007)**	ATTTCTTTTCACCGTTAACAAGGCG	5' UTR-ATG	1.4 mM
***rap1b* (Tsai et al. 2007)**	ACGCATTGTGCAGTGTGTCCGTTAA	5' UTR-ATG	600 µM
***rap1b-2* (Tsai et al. 2007)**	CAATAGAAATGATGCAGAACTTGCC	Intron 2	1.6 mM
rapGEF-2	CTCCGAGTTCATCTGTTGCAGCAAC	5' UTR-ATG	1.6 mM
rapGEF	TCAGCCCACTTACCCAGCTGATTCC	Intron 1	300 µM
***ephrinb2a* (Koshida et.al. 2005)**	AATATCTCCACAAAGAGTCGCCCAT	5'UTR-ATG	900 µM

Table 5

Sequences and binding sites of morpholinos used in this study.
The concentration at which each morpholino was injected is also indicated.

4.11. Image acquisition

Standard *in situ* hybridisation images were captured using a Zeiss Stemi SV6 dissecting scope and Leica FireCam DFC 300 software. Wide field DIC images were collected using a 20x objective on a Zeiss Axioskop 2 mot (*plus*) and Openlab software. Confocal images were acquired using a 40x objective on a Zeiss LSM 510 and Zen2008 software. Images were processed using Adobe Photoshop CS3 and ImageJ. Figures were created using Adobe Illustrator CS3.

5. Appendix

5.1. *rapGEF* ZF coding sequence

ATGCATCTCTTTCGGAGTTACAATTACAAAGTCTTTCCCGATCGTTGTTCCAATGA
GAAAACTCCTCAGATTCGGGGAAT
CAGCTGGACGCCTCTGCCAGACGCTGTGGATACACAAGACACCATCAAACAGTTT
TTATCAGATCGAATCCTGAAGGCTG
CACGGGTAGTTTACAGCACTCTGATGGAGGGTAACCCAGGCCTGATAAGAGACA
GAAAACACCATCTTAAGACCTACAGA
CAGTGCTGCAGCGGAAAGGAGCTTGTGGATTGGTTAATGAAACTCAATGATTGTT
TCCAGTCCCGGAGTCAGGCAGTCGG
AATGTGGCAGGTTTTGGTGGATGAGGGCATTTTGGGTCATGTAAAACAGGAGTTA
AACTTCCATGACAAAGACACACAGT
TTTACCGCTTTATGGAAGCAGAGTTTGACCTCAATCACACAACTAACGAAAAAGA
CTCCAAAGACGACGAACTACAAGAG
AGTTTATCGCTACTAATCCAGATGGGCCCAGATGCTCTTTTGACGATGATACTGC
GTAAATGCCCAAGCCAGAGAACCCC
AGAAGATCTGGAAGTTATTTATGAAGAACTTCTGCACGTCAAAGCTGTGGCCCAC
TTGTCTACATCTGTTCGTAAAGAGC
TGGCATCAGTGCTGGTATTTGAAAGCCATGCCAAGGCGGGAACAGTCTTGTTCAG
TCAGGGGGACAAAGGGACTTCCTGG
TACATCATCTGGAGAGGCTCTGTTAATGTCATCACACACGGCAAGGGCTTGGTGA
CTACGCTTCATGAAGGAGATGATTT
TGGCCAGTTGGCATTGGTGAATGACGCTCCTCGAGCCGCCACCATCATTTTAAGA
GAGGACAATTGCCACTTTCTGCGGG
TGGACAAGCAGGATTTTATACGCATTCTTAAGGACGTCGAGGCAAACACCGTCCG
TCTGGAGGAGCATGGTAAAGTCGTT
CTGGTTCTTGAGAAGAGCTCGGCGCAGGATACACCAAGCTGCAACAAGTACACG
GTAATGTCAGGAACGCCGGAAAAGAT
CCTGGAGCACATGCTGGAGGCCATAAAACTGGAAACCAACGGAGCTGACTTCAT
AGATCCCTGTGTGACTGACTTTCTCC
TAACGCATCCCGTCTTCATGCCCTGCAGTCAACTGTGTGCTGCCCTCCAGCATCAT
TACCAAGCGGAGCCGTCTGAAGGC
TCAGACCTGGAGAAGGCAGCGTACGCTCTCAACACCAAGCAGAAGGTGGTGAAG
CTGGTGTGTCACTGGGTGGCTCTGTT
CGCTCTGCTGCTCAGGGACGATCCTGTGGCCTCTGAATTCCTGGAGAAATTCAGG
GAAGGAGTGATGGCAGACTCAAGAC
TTTCTAGCATGCTTAGAGAACAGCTAAGGGACAGGAGGAAGACAAAAATAATGG
AGAATGGATGTCACACTCTGACAAAG
CTGAACCAAAAGTTTGATTGGTTTTCAGCTTACGAAGAGCCGGTGGGAAAACTGA
GGTCGATTAAAGCCCAAGATAAAGT
GTTGTATGAGATCTTTAAACCGGATCATAAGGCTGTCACTGTGATGCTGCCAGTT
GATGCATCGGTGAACGACATCTTGA

CTACATTAGTGGATCCTGACAGAAACTATGTGCTTGTCAAGATGAATTCCTCAGG
AGACAGAGTCCAGCTGAAGTTGGAG
ACCACAGCAGTGTCTGCCTCTTTAGGAGTGAACGAAAAGCTTTTCCTCTGCACTT
CCAGCCAAGTTGAACAACTGACACC
TGATAAAGAGCAGCTGGGGCCGGAGAAGAGCACCATGGACACTCTGGAGCAGAT
TTGCTCCAAGGACATGGCCAGTCAAC
ACACCAGCTACGACTGGGAACTCTTCATGGCCATGCATGAGGTGGAGCTTGTCTA
CTATGTTTTCGGACGGGAAAAGTTC
CCTGGATCCACCACAGCAAACCTCGAGCGGTTTGTTCGTCGCTTCAATGAGGTTC
AGTACTGGGTTGTGACTGAACTGTG
TCTCTGTGAAGACCTGGGCAAGAGAGCCATACTGCTGAAGAAGTTCATCAAGAT
GGCTGTTGTTTTGAAAGAGCAGAAGA
ACCTCAACTCTTTTTTCGCAGTAATGTTTGGCCTCAGCAACAGTGCAGTGCAGAG
GCTCAATAAAACATGGGAGAGACTT
CCCAATAAAACCAAAAGGATCTACTGTGCATACGAAAGACTGATGGATCCGTCC
CGTAACCACAGGGCCTACAGACTGAC
TATTGCCAAACTCAGCCCTCCATACATTCCCTTCATGCCACTGCTTCTAAAAGATA
TGACATTTATTCATGAGGGAAACA
AGAACTACACTGATAAACTGGTCAACTTTGAGAAAATGCGCATGATTGCCAGAA
CAGTGAAGACAGTTCGGGATTGTCGA
AGCCAACCTTACGTGCCTTCATCTCCGCAGAAAGGCTTGACGGAGAGAATGTTCT
TGGATGCTCAAGCTATCCGAATATC
AACATATTCAGACCAGTCTCTGAACCTCCGCAGTGCCACCAGTATCAGACAGTAC
ATCCAGAACCTGAAAGTGATCGACA
ATCAGAAGAAACTAACTCAGCTCTCCAGAGCCTTAGAGCGCTGA

5.2. RapGEF ZF protein sequence

MHLFRSYNYKVFPDRCSNEKTPQIRGISWTPLPDAVDTQDTIKQFLSDRILKAARVVY
STLMEGNPGLIRDRKHHLKTYR
QCCSGKELVDWLMKLNDCFQSRSQAVGMWQVLVDEGILGHVKQELNFHDKDTQF
YRFMEAEFDLNHTTNEKDSKDDELQE
SLSLLIQMGPDALLTMILRKCPSQRTPEDLEVIYEELLHVKAVAHLSTSVRKELASVL
VFESHAKAGTVLFSQGDKGTSW
YIIWRGSVNVITHGKGLVTTLHEGDDFGQLALVNDAPRAATIILREDNCHFLRVDKQ
DFIRILKDVEANTVRLEEHGKVV
LVLEKSSAQDTPSCNKYTVMSGTPEKILEHMLEAIKLETNGADFIDPCVTDFLLTHPV
FMPCSQLCAALQHHYQAEPSEG
SDLEKAAYALNTKQKVVKLVCHWVALFALLLRDDPVASEFLEKFREGVMADSRLSS
MLREQLRDRRKTKIMENGCHTLTK
LNQKFDWFSAYEEPVGKLRSIKAQDKVLYEIFKPDHKAVTVMLPVDASVNDILTTLV
DPDRNYVLVKMNSSGDRVQLKLE
TTAVSASLGVNEKLFLCTSSQVEQLTPDKEQLGPEKSTMDTLEQICSKDMASQHTSY
DWELFMAMHEVELVYYVFGREKF
PGSTTANLERFVRRFNEVQYWVVTELCLCEDLGKRAILLKKFIKMAVVLKEQKNLNS
FFAVMFGLSNSAVQRLNKTWERL

PNKTKRIYCAYERLMDPSRNHRAYRLTIAKLSPPYIPFMPLLLKDMTFIHEGNKNYTD
KLVNFEKMRMIARTVKTVRDCR
SQPYVPSSPQKGLTERMFLDAQAIRISTYSDQSLNLRSATSIRQYIQNLKVIDNQKKLT
QLSRALER

5.3. *rap1b* ZF coding sequence

ATGCGTGAATACAAGTTAGTAGTCCTCGGATCAGGAGGTGTTGGCAAGTCTGCGC
TG**ACTGTTCAATTTGTCCAAGGGAT**
CTTTGTGGAGAAGTATGACCCTACAATAGAAGACTCGTACAGAAAGCAAGTG
GAGGTGGATGGACAGCAGTGTATGTTGG
AAATTCTGGATACTGCCGGAACGGAACAATTCACAGCCATGAGGGACCTGTACA
TGAAGAACGGCCAGGGCTTTGCACTA
GTTTACTCCATAACAGCACAGTCCACCTTCAACGACCTGCAGGACTTGAGAGAAC
AAATTCTGCGGGTGAAAGACACAGA
TGATGTGCCGATGATCCTGGTGGGCAATAAGTGTGATCTGGAGGACGAGAGGGT
GGTGGGCAAGGAGCAGGGGCAGAATC
TTGCCCGGCAGTGGAACAGCTGCGCCTTTCTGGAGTCCTCCGCAAAATCCAAGAT
TAACGTCAATGAGATTTTCTATGAC
CTGGTCCGGCAAATCAACAGGAAAACTCCAGTAACTGGAAAGCCACGCAAAAAG
TCCACCTGCCAGTTGCTCTAA

5.4. *rap1b* ZF coding sequence of an altered splice product after *rap1b-2* MO injection

The sequence of the altered splice product of rap1b misses the complete second exon, the red labeled sequence in 5.3.

ATGCGTGAATACAAGTTAGTAGTCCTCGGATCAGGAGGTGTTGGCAAGTCTGCGC
TGCAAGTGGAGGTGGATGGACAGCA
GTGTATGTTGGAAATTCTGGATACTGCCGGAACGGAACAATTCACAGCCATGAGG
GACCTGTACATGAAGAACGGCCAGG
GCTTTGCACTAGTTTACTCCATAACAGCACAGTCCACCTTCAACGACCTGCAGGA
CTTGAGAGAACAAATTCTGCGGGTG
AAAGACACAGATGATGTGCCGATGATCCTGGTGGGCAATAAGTGTGATCTGGAG
GACGAGAGGGTGGTGGGCAAGGAGCA
GGGGCAGAATCTTGCCCGGCAGTGGAACAGCTGCGCCTTTCTGGAGTCCTCCGCA
AAATCCAAGATTAACGTCAATGAGA
TTTTCTATGACCTGGTCCGGCAAATCAACAGGAAAACTCCAGTAACTGGAAAGCC
ACGCAAAAAGTCCACCTGCCAGTTG
CTCTAA

5.5. Rap1b ZF protein sequence

MREYKLVVLGSGGVGKSAL**TVQFVQGIFVEKYDPTIEDSYRK**QVEVDGQQCMLEI
LDTAGTEQFTAMRDLYMKNGQGFAL
VYSITAQSTFNDLQDLREQILRVKDTDDVPMILVGNKCDLEDERVVGKEQGQNLAR
QWNSCAFLESSAKSKINVNEIFYD
LVRQINRKTPVTGKPRKKSTCQLL

5.6. Rap1b ZF protein sequence of an altered splice product after *rap1b-2* MO injection

MREYKLVVLGSGGVGKSALQVEVDGQQCMLEILDTAGTEQFTAMRDLYMKNGQGF
ALVYSITAQSTFNDLQDLREQILRV
KDTDDVPMILVGNKCDLEDERVVGKEQGQNLARQWNSCAFLESSAKSKINVNEIFY
DLVRQINRKTPVTGKPRKKSTCQLL

5.7. Gene-specificity of splice-blocking morpholino *rap1b-2*

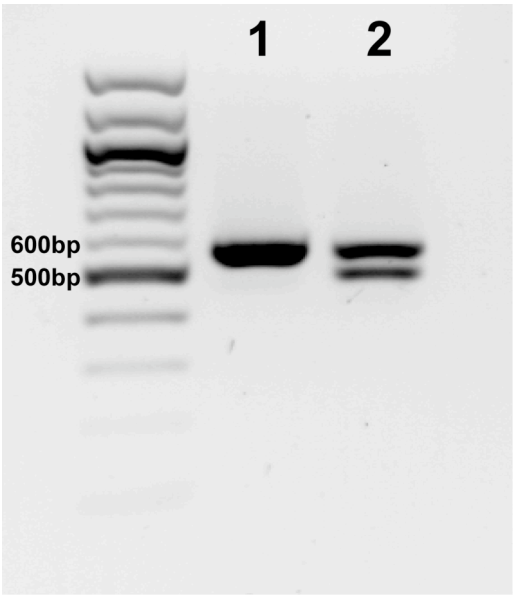

Lane 1 shows the PCR product of wild-type *rap1b* cDNA.
Lane 2 shows the PCR product of wild-type *rap1b* cDNA and the altered splice product generated vie splice-blocking morpholino *rap1b-2*, which is about 70bp smaller than the wild-type *rap1b* cDNA.

6. Abbreviations

amp	ampicillin
BAC	bacterial artificial chromosome
bp	base pairs
bfe	before eight
cDNA	complementary DNA
BMP	bone morphogenetic protein
ECM	extracellular matrix
EDTA	ethylenediaminetetraacetic acid
DIC	differential interference contrast
DIG	digoxigenin
DMSO	dimethyl sulfoxide
DN	dominant negative
DNA	deoxyribonucleic acid
dNTP	deoxyribonucleotide triphosphate
DTT	dithiothreitol
GAP	GTPase-activating protein
GEF	guanine-nucleotide exchange factor
GFP	green fluorescent protein
GTP	guanosine triphosphate
GDP	guanosine diphosphate
hpf	hours past fertilisation
HF	high fidelity
kbp	kilo base pairs
LB	luria-bertani
MET	mesenchymal-to-epithelial transition
MMLV	murine leukemia virus
mRNA	messenger ribonucleic acid
MO	morpholino
NEB	New England Biolabs
NUP	nested universal primer
PBS	phosphate buffered saline

PCR	polymerase chain reaction
PFA	paraformaldehyde
PSM	presomitic mesoderm
RACE	rapid amplification of cDNA ends
RNA	ribonucleic acid
RT	room temperature
SDS	sodium dodecyl sulfate
TE	Tris-EDTA
fgf	fibroblast growth factor
UTR	untranslated region
UPM	universal primer mix
ZF	zebrafish

7. References

Abraham T.R (2003) *Rap1 redux*. Nature Immunology 4:725-727

Aoki et al. (2004). EphA4 Receptors Direct the Differentiation of Mammalian Neural Precursor Cells through a Mitogen-activated Protein Kinase-dependent Pathway. The Journal of biological Chemestry 279, 32643-32650

Asha et al. (1999). The Rap1 GTPase functions as a regulator of morphogenesis in vivo. The EMBO Journal 18, 605-615

Barrios et al. (2003). Eph/Ephrin Signaling Regulates the Mesenchymal-to-Epithelial Transition of the Paraxial Mesoderm during Somite Moprhogenesis. Current Biology 13, 1571-1582

Brand et al. (2002). Keeping and raising zebrafish. In: Nüsslein-Volhard C., Dahm R., editors. Zebrafish. New York: Oxford University Press 7-37

Bos et al. (2001). Rap1 signalling: adhering to new models. Nature Reviews, Molecular Cell Biology 2, 369-377

Cooke and Zeeman (1976). A Clock and Wavefront Model for Control of the Number of Repeated Structures during Animal Morphogenesis. J. theor. Biol. 58, 455-476

Cooke et al. (2001). Eph signalling functions downstream of Val to regulate cell sorting and boundary formation in the caudal hindbrain. Development 128, 571-580

Dubrulle et al. (2001). FGF Signaling Controls Somite Boundary Position and Regulates Segmentation Clock Control of Spatiotemporal *Hox* Gene Activation. Cell 106, 219-232

Durbin et al. (1998). Eph signalling is required for segmentation and differentiation of the somites. Genes Dev. 12, 3096-3109

Durbin et al. (2000). Anteroposterior patterning is required within segments for somite boundary formation in developing zebrafish. Development 127, 1703-1713

Gabig et al. (1995). Function of Wild-Type or Mutant Rac2 and Rap1a GTPases in Differential HL60 Cell NADPH Oxidase Activation. Blood 85, 804-811

Gomez et al. (2008). Control of segment number in vertebrate embryos. Nature 454, 335-339

Gore et al. (2008). Combinatorial interaction between CCM pathway genes precipitates hemorrhagic stroke. Disease Models & Mechanisms 1, 275-281

George et al. (1993). Defects in mesoderm, neural tube and vascular development in mouse embryos lacking fibronectin. Development 119; 1079-1091

Holley et al. (2000). Control of her1 expression during zebrafish somitogenesis by a Delta-dependent oscillator and an independent wave-front activity. Genes & Dev. 14, 1678-1690

Holley et al. (2002). *her1* and the *notch* pathway function ithin the oscillator mechanism that regulates zebrafish somitogenesis. Development 129, 1175-1183

Huynh-Do et al. (1999). Surface densities of Ephrin-B1 determine EphB1-coupled activation of cell attachment through $\alpha_v\beta_3$ and $\alpha_5\beta_1$ integrins. The EMBO Journal 18, 2165-2173

Hynes (1994). Genetic analyses of cell-matrix interactions in development. Curr Opin Genet Dev 4, 569-574

Jülich et al. (2005a). Integrinα5 and Delta/Notch Signaling have Complimentary Spatiotemporal requirements during Zebrafish Development. Developmental Cell 8, 575-586

Jülich et al. (2005b). *beamter/deltaC* and the role of Notch ligands in the zebrafish somite segmentation, hindbrain neurogenesis and hypochord differentiation. Dev Biol 286, 391-404

Jülich (2005c). Genetic analysis of difference in the spatiotemporal control of somitogenesis in the zebrafish, *Danio rerio*. Fakultät für Biologie der Eberhard Karls Universität Tübingen

Kanki and Ho (1997). The development of the posterior body in zebrafish. Development 124, 881-893

Katagiri et al. (2003). RAPL, a Rap1-binding molecule that mediates Rap 1 induced adhesion through spatial regulation of LFA-1. Nature Immunology 4, 741-748

Kawamura et al. (2005). Groucho-Associated Transcriptional Repressor Ripply1 is Required for Proper Transition from the Presomitic Mesoderm to Somites. Developmenatl Cell 9, 735-744

Kimmel et al. (1995). Stages of Embryonic Development of the Zebrafish. Developmental Dynamics 203, 253-310

Kinbara et al. (2003). Ras GTPases: Integrins' friends or foes? Nature Review, Molecular Cell Biology 4, 767-776

Knox and Brown (2002). Rap1 GTPase Regulation of Adherens Junction Positioning and Cell Adhesion. Science 295, 1285-1288

Koshida et al. (2005). Integrinα5-Dependent Fibronectin Accumulation for Maintenance of Somite Boundaries in Zebrafish Embryos. Developmental Cell 8, 587-598

Mao and Schwarzbauer (2005). Fibronectin fibrillogenesis, a cell-mediated matrix assembly process. Matrix Biology 24, 389-399

Mara (2008). Differential delta signaling during zebrafish somitogenesis and midline development. Faculty of the Graduate School of Yale University

Mellitzer et al. (1999). Eph receptors and ephrins restrict cell intermingling and communication. Nature 400, 77-81

Myers et al. (2002). Bmp Activity Gradient Regulates Convergent Extension during Zebrafish Gastrulation. Developmental Biology 243, 81-98

Nüsslein-Volhard and Dahm, Eds (2002) Zebrafish. Practical Approach.Oxford, UK, Oxford University Press.

Palmeirim et al. (1997). Avian *hairy* Gene Expression Identifies a Molecular Clock Linked to Vertebrate Segmentation and Somitogenesis. Cell 91, 639-648

Pasquale (2005). Eph receptor signalling casts a wide net on cell behaviour. Nat. Rev. Mol. Cell Biol. 6, 462-475

Pasquale (2008). Eph-Ephrin Bidirectional Signaling in Physiology and Disease. Cell 133, 38-52

Pourquie (2001). Vertebrate Somitogenesis. Annu Rev. Cell Dev. Biol. 17, 311-350

Price et al. (2004). Rap1 regulates E-cadherin-mediated cell-cell adhesion. J Biol Chem 279, 35127-35132

Richardson et al. (1998). Somite number and vertebrate evolution. Development 125, 151-160

Sambrook and Russell (2001). Molecular Cloning-A Laboratory Manual. New York: Cold Spring Harbor Laboratory Press

Saga and Takeda (2001). The making of the somite: Molecular events in vertebrate segmentation. Nature Reviews Genetics 2, 835-845

Sawada et al. (2000). Zebrafish *Mesp* family genes, *mesp-a* and *mesp-b* are segmentally expressed in the presomitic mesoderm, and Mesp-b confers the anterior identity to the developing somites. Development 127, 1691-1702

Sawada et al. (2001). Fgf/MAPK signalling is a crucial positional cue in somite boundary formation. Development 128, 4873-4880

Schier (2003). Nodal Signaling in Vertebrate Development. Annu. Rev. Cell Dev. Biol. 19, 589-621

Schwarzbauer and Sechler (1999). Fibronectin fibrillogenesis: a paradigm for extracellular matrix assembly. Current Opinion in Cell Biology 11, 622-627

Sebzda et al. (2002). Rap1A positively regulates T cells via Integrin activation rather than inhibiting lymphocyte signalling. Nature Immunology 3, 251-258

Sonnenberg (1993). Integrins and their ligands. Curr Top Micor Immun. 184, 7-35

Song et al. (2004). Hematopoietic gene expression profile in zebrafish kidney marrow. Proc. Natl. Acad. Sci. USA 101, 16240-16245

Strausberg et al. (2002). Generation and initial analysis of more than 15,000 full-length human and mouse cDNA sequences. Proc. Natl. Acad. Sci. 99, 16899-903

Szeto and Kimelman (2006). The regulation of mesodermal progenitor cell commitment to somitogenesis subdivides the zebrafish body musculature into distinct domains. Genes & Development 20, 1923-1932

Thisse et al. (2001).Expression of the zebrafish genome during embryogenesis (NIH R01 RR15402). ZFIN Direct Data Submission (http://zfin.org).

Tsai et al. (2007). A Wnt-CKIε-Rap1 Pathway Regulates Gastrulation by Modulating SIPA1L1 a Rap GTPase Activating Protein. Dev Cell 12, 335-347

Van Eeden et al. (1996). Mutations affecting somite formation and patterning in the zebrafish, *Danio rerio*. Development 123, 153-164

Xu et al. (1995). Expression of truncated Sek-1 receptor tyrosine kinase disrupts the segmental restriction of gene expression in the Xenopus and zebrafish hindbrain. Development 121, 4005-40016

Curriculum Vitae

Name:	Simone Lackner
Email:	Lackner_simone@yahoo.de
Date of Birth:	22.July.1984
Place of Birth:	Klosterneuburg, Austria

Education:

1994-2002	Wirtschaftkundliches-Realgymnasium Kenyongasse "Mater Salvatoris"
2002	Matura (*High-School-Diploma*)
2002-2009	Faculty of Molecular Biology at the University of Vienna Magistra der Naturwissenschaften

Laboratory Experience:

June 2003	Food Quality Control Laboratory LVA –Vienna; Dr. Leopold Reiner Microbiological analysis of food Summer practical
September 2004-June 2005	Clinical Institute of Medical-Chemical Diagnostics at AKH Vienna Research Project in Molecular Pathology Prof. Dr. Mannhalter Development of mutagenetically separated PCR methods to detect genetic polymorphism in stroke patients Scientific Assistant
July 2005	Austrian Research Center ARC Seibersdorf Research GmbH Dr. Maria Berenyi Functional genomics for the elucidation of *beta*-carotene and starch metabolism in sweet potato Optimization of the binding of TempliPhi amplified plasmid DNA on Clone Saver Card Summer practical

September 2005-June 2006	Institute of Molecular Pathology - Vienna Dr. Barry J. Dickson Dissecting the role of *fruitless* in *Drosophila* male sexual behavior Technical Assistant
August 2006-February 2007	Temasek Lifesciences Laboratory - Singapore Prof. Dr. William Chia Characterization of proteins involved in asymmetric cell division of the *Drosophila* neuroblast Internship
October – November 2007	Max F. Perutz Laboratories – Vienna Prof. Dr. Timothy Skern Viral Proteinases Wahlbeispiel (*Compulsory University practical*)
March 2008 – Mai 2009	Department of Molecular, Cellular and Developmental Biology Yale University – USA Prof. Dr. Scott Holley Genetic Analysis of Rap1 GTPase Function in Vertebrate Axis Extension and Somitogenesis Diplomarbeit (*Master thesis*)

Technical assistance:

Rita Sousa-Nunes, William Chia and W. Greg Somers (2009)
Protein Phosphatase 4 mediates localization of the Miranda complex during *Drosophila* neuroblast asymmetric division
Genes Dev. 23: 359-372

Poster Price:

Simone Lackner, Dörthe Jülich and Scott A. Holley
'Genetic analysis of Rap1 GTPase function in zebrafish somitogenesis'
MCDB Retreat 2008, Woods Hole (MA)

Languages:	German English